

Singlet vs Nonsinglet Perturbative Renormalization of Fermion Bilinears

M. Constantinou^{a,b}, M. Hadjiantonis^{a,c}, H. Panagopoulos^a and G. Spanoudes^{a*}

^a *Department of Physics, University of Cyprus, POB 20537, 1678 Nicosia, Cyprus*

^b *Present address: Department of Physics, Temple University, Philadelphia, PA 19122 – 1801, USA*

^c *Present address: Department of Physics, University of Michigan, Ann Arbor, MI 48109, USA*

In this paper we present the perturbative evaluation of the difference between the renormalization functions of flavor singlet and nonsinglet bilinear quark operators on the lattice. The computation is performed to two loops and to lowest order in the lattice spacing, for a class of improved lattice actions, including Wilson, tree-level (TL) Symanzik and Iwasaki gluons, twisted mass and SLiNC Wilson fermions, as well as staggered fermions with twice stout-smearred links. In the staggered formalism, the stout smearing procedure is also applied to the definition of bilinear operators.

I. INTRODUCTION

In this work we study the renormalization of fermion bilinears $\mathcal{O}_\Gamma = \bar{\psi}\Gamma\psi$ on the lattice, where $\Gamma = \mathbb{1}, \gamma_5, \gamma_\mu, \gamma_5 \gamma_\mu, \gamma_5 \sigma_{\mu\nu}$ ($\sigma_{\mu\nu} = [\gamma_\mu, \gamma_\nu]/2i$). We consider flavor singlet ($\sum_f \bar{\psi}_f \Gamma \psi_f$, f : flavor index) as well as nonsinglet ($\bar{\psi}_{f_1} \Gamma \psi_{f_2}$, $f_1 \neq f_2$) operators, to two loops in perturbation theory. More specifically, we compute the difference between the renormalization functions of singlet and nonsinglet operators. Our calculations were performed making use of a large family of lattice actions, including Symanzik improved gluons, Wilson and staggered fermions with stout links, and clover fermions; twisted mass actions (with Iwasaki or tree-level Symanzik gluons) and the SLiNC action are members of this family. This work is a continuation to our conference paper [1], in which we presented our perturbative results using Wilson/clover fermions.

The most demanding part of this study is the computation of the 2-point Green's functions of \mathcal{O}_Γ , up to two loops. From these Green's functions we extract the renormalization functions for \mathcal{O}_Γ : $Z_\Gamma^{L,Y}$ (L : lattice regularization, Y ($= RI', \overline{MS}$): renormalization schemes). As a check on our results, we have computed them in an arbitrary covariant gauge. Our expressions can be generalized, in a straightforward manner, to fermionic fields in an arbitrary representation.

Flavor singlet operators are relevant for a number of hadronic properties including, e.g., topological features or the spin structure of hadrons. Matrix elements of such operators are notoriously difficult to study via numerical simulations, due to the presence of (fermion line) disconnected diagrams, which in principle require evaluation of the full fermion propagator. In recent years there has been some progress in the numerical study of flavor singlet operators; furthermore, for some of them, a nonperturbative estimate of their renormalization has been obtained using the Feynman-Hellmann relation [2]. Perturbation theory can give an important cross check for these estimates, and provide a prototype for other operators which are more difficult to renormalize nonperturbatively.

Given that for the renormalization of flavor nonsinglet operators one can obtain quite accurate nonperturbative estimates, we will focus on the perturbative evaluation of the *difference* between the flavor singlet and nonsinglet renormalization; this difference first shows up at two loops.

Perturbative computations beyond one loop for Green's functions with nonzero external momenta are technically quite involved, and their complication is greatly increased when improved gluon and fermion actions are employed. For fermion bilinear operators, the only two-loop computations in standard perturbation theory thus far have been performed by our group [3, 4], employing Wilson gluons and Wilson/clover fermions. Similar investigations have been carried out in the context of stochastic perturbation theory [5].

Staggered fermions entail additional complications as compared to Wilson fermions. In particular, the fact that fermion degrees of freedom are distributed over neighbouring lattice points requires the introduction of link variables in

*Electronic address: marthac@temple.edu, mhadjian@umich.edu, haris@ucy.ac.cy, spanoudes.gregoris@ucy.ac.cy

the definition of gauge invariant fermion bilinears, with a corresponding increase in the number of Feynman diagrams. In addition, the appearance of 16 (rather than 1) poles in the fermion propagator leads to a rather intricate structure of divergent contributions in two-loop diagrams.

A novel aspect of the calculations is that the gluon links, which appear both in the staggered fermion action and in the definition of the bilinear operators in the staggered basis, are improved by applying a stout smearing procedure up to two times, iteratively. Compared to most other improved formulations of staggered fermions, the stout smearing action leads to smaller taste violating effects [6–8]. Application of stout improvement on staggered fermions thus far has been explored, by our group, only to one-loop computations [9]; a two-loop computation had never been investigated before.

Further composite fermion operators of interest, to which one can apply our perturbative techniques, are higher dimension bilinears such as: $\bar{\psi}\Gamma D^\mu\psi$ (appearing in hadron structure functions) and four-fermion operators such as: $(\bar{s}\Gamma_1 d)(\bar{s}\Gamma_2 d)$ (appearing in $\Delta S = 2$ transitions, etc.); in these cases, complications such as operator mixing greatly hinder nonperturbative methods of renormalization, making a perturbative approach all that more essential.

The outline of this paper is as follows: Section II presents a brief theoretical background in which we introduce the formulation of the actions and of the operators which we employ, as well as all necessary definitions of renormalization schemes and of the quantities to compute. Section III contains the calculational procedure and the results which are obtained. In Section IV we discuss our results and we plot several graphs for certain values of free parameters, like the stout and clover coefficients. Finally, we conclude with possible future extensions of our work. For completeness, we have included two Appendices containing: A: the formulation of the fermion action and the bilinear operators in the staggered basis, along with a compendium of useful relations and B: evaluation of a basis of nontrivial divergent two-loop Feynman diagrams, which appeared in our calculation in the staggered formalism.

II. FORMULATION

A. Lattice actions

In our calculation we made use of two totally different formulations of the fermion action on the lattice: Wilson and staggered formulation. In the Wilson formulation, we used the SLiNC fermion action [10], i.e., we introduced stout gluon links in the standard Wilson action and also we added the clover term. In standard notation, it reads:

$$\begin{aligned}
S_{\text{WF}} = & -\frac{a^3}{2} \sum_{x,\mu} \bar{\psi}(x) \left[(r - \gamma_\mu) \tilde{U}_\mu(x) \psi(x + a\hat{\mu}) + (r + \gamma_\mu) \tilde{U}_\mu^\dagger(x - a\hat{\mu}) \psi(x - a\hat{\mu}) - 2r \psi(x) \right] \\
& - \frac{a^5}{4} \sum_{x,\mu,\nu} c_{\text{SW}} \bar{\psi}(x) \sigma_{\mu\nu} \hat{G}_{\mu\nu}(x) \psi(x)
\end{aligned} \tag{1}$$

where

$$\hat{G}_{\mu\nu}(x) = \left[Q_{\mu\nu}(x) - Q_{\nu\mu}(x) \right] / (8a^2) \tag{2}$$

and

$$\begin{aligned}
Q_{\mu\nu} = & U_\mu(x) U_\nu(x + a\hat{\mu}) U_\mu^\dagger(x + a\hat{\nu}) U_\nu^\dagger(x) \\
& + U_\nu(x) U_\mu^\dagger(x + a\hat{\nu} - a\hat{\mu}) U_\nu^\dagger(x - a\hat{\mu}) U_\mu(x - a\hat{\mu}) \\
& + U_\mu^\dagger(x - a\hat{\mu}) U_\nu^\dagger(x - a\hat{\mu} - a\hat{\nu}) U_\mu(x - a\hat{\mu} - a\hat{\nu}) U_\nu(x - a\hat{\nu}) \\
& + U_\nu^\dagger(x - a\hat{\nu}) U_\mu(x - a\hat{\nu}) U_\nu(x + a\hat{\mu} - a\hat{\nu}) U_\mu^\dagger(x)
\end{aligned} \tag{3}$$

The fermion action may also contain standard and twisted mass terms, but they only contribute beyond two loops to the difference between flavor singlet and nonsinglet renormalizations; this is true in mass-independent schemes, such

as RI' and \overline{MS} , in which renormalized masses vanish. The quantities $\tilde{U}_\mu(x)$, appearing above, are stout gluon links, defined as [11]:

$$\tilde{U}_\mu(x) = e^{iQ_\mu(x)} U_\mu(x) \quad (4)$$

where

$$Q_\mu(x) = \frac{\omega}{2i} \left[V_\mu(x) U_\mu^\dagger(x) - U_\mu(x) V_\mu^\dagger(x) - \frac{1}{N_c} \text{Tr} \left(V_\mu(x) U_\mu^\dagger(x) - U_\mu(x) V_\mu^\dagger(x) \right) \right] \quad (5)$$

$V_\mu(x)$ represents the sum over all staples associated with the link $U_\mu(x)$ and N_c is the number of colors. Following common practice, we henceforth set the Wilson parameter r equal to 1. Both the stout coefficient ω and the clover coefficient c_{SW} will be treated as free parameters, for wider applicability of the results.

In the staggered formulation of fermion action, we introduced “doubly” stout gluon links in the naive staggered action. In standard notation, it reads:

$$S_{\text{SF}} = a^4 \sum_{x,\mu} \frac{1}{2a} \bar{\chi}(x) \eta_\mu(x) \left[\tilde{\tilde{U}}_\mu(x) \chi(x + a\hat{\mu}) - \tilde{\tilde{U}}_\mu^\dagger(x - a\hat{\mu}) \chi(x - a\hat{\mu}) \right] + a^4 \sum_x m \bar{\chi}(x) \chi(x) \quad (6)$$

where $\chi(x)$ is a one-component fermion field, and $\eta_\mu(x) = (-1)^{\sum_{\nu < \mu} n_\nu}$ [$x = (a n_1, a n_2, a n_3, a n_4)$, $n_i \in \mathbb{Z}$]. Just as in the case of Wilson fermions, the mass term will be irrelevant, since we will apply mass-independent renormalization schemes. In Appendix A we remind the reader of the relation between the staggered field $\chi(x)$ and the standard fermion field $\psi(x)$. The gluon links $\tilde{\tilde{U}}_\mu(x)$, appearing above, are doubly stout links, defined as:

$$\tilde{\tilde{U}}_\mu(x) = e^{i\tilde{Q}_\mu(x)} \tilde{U}_\mu(x) \quad (7)$$

where $\tilde{U}_\mu(x)$ is the singly stout link, defined in Eq. (4) and $\tilde{Q}_\mu(x)$ is defined as in Eq.(5), but using \tilde{U}_μ as links (also in the construction of V_μ). To obtain results that are as general as possible, we use different stout parameters, ω , in the first (ω_1) and the second (ω_2) smearing iteration.

For gluons, we employ a Symanzik improved action, of the form [12]:

$$S_G = \frac{2}{g_0^2} \left[c_0 \sum_{\text{plaq.}} \text{Re Tr} \{1 - U_{\text{plaq.}}\} + c_1 \sum_{\text{rect.}} \text{Re Tr} \{1 - U_{\text{rect.}}\} + c_2 \sum_{\text{chair}} \text{Re Tr} \{1 - U_{\text{chair}}\} + c_3 \sum_{\text{paral.}} \text{Re Tr} \{1 - U_{\text{paral.}}\} \right] \quad (8)$$

where $U_{\text{plaq.}}$ is the 4-link Wilson loop and $U_{\text{rect.}}$, U_{chair} , $U_{\text{paral.}}$ are the three possible independent 6-link Wilson loops

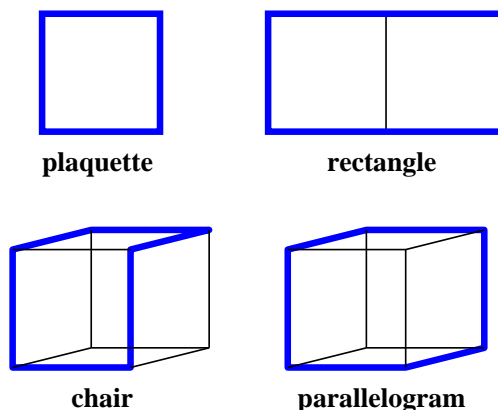


FIG. 1: The 4 Wilson loops of the gluon action.

(see Fig. 1). The Symanzik coefficients c_i satisfy the following normalization condition:

$$c_0 + 8c_1 + 16c_2 + 8c_3 = 1 \quad (9)$$

The algebraic part of our computation was carried out for generic values of c_i ; for the numerical integration over loop momenta we selected a number of commonly used sets of values, some of which are shown in Table I. We have also performed our calculations for some other values of c_i , relevant to the TILW (tadpole improved Lüscher - Weisz) family of actions.

Gluon action	c_0	c_1	c_2	c_3
Wilson	1	0	0	0
TL Symanzik	5/3	-1/12	0	0
Iwasaki	3.648	-0.331	0	0
DBW2	12.2688	-1.4086	0	0

TABLE I: Selected sets of values for Symanzik coefficients

B. Definition of bilinear operators in the staggered basis

In the staggered formalism a physical fermion field $\psi(x)$ has “taste” components, besides Dirac components (see Appendix A). Hence, the fermion bilinear operators, written in terms of fermion fields with taste $\psi_{\alpha,t}(x)$ (α : Dirac index, t : taste index), have the following form:

$$\mathcal{O}_{\Gamma,\xi} = \bar{\psi}(x) (\Gamma \otimes \xi) \psi(x) \quad (10)$$

where Γ and ξ are arbitrary 4×4 matrices acting on the Dirac and taste indices of $\psi_{\alpha,t}(x)$, respectively. After transforming to the staggered basis, the operator $\mathcal{O}_{\Gamma,\xi}$ can be written as [13]:

$$\mathcal{O}_{\Gamma,\xi} = \sum_{C,D} \bar{\chi}(y)_C (\overline{\Gamma \otimes \xi})_{CD} U_{C,D} \chi(y)_D, \quad (11)$$

$$(\overline{\Gamma \otimes \xi})_{CD} \equiv \frac{1}{4} \text{Tr} [\gamma_C^\dagger \Gamma \gamma_D \xi] \quad (12)$$

where $\chi(y)_C \equiv \chi(y + aC)/4$ [y denotes the position of a hypercube inside the lattice ($y_\mu \in 2\mathbb{Z}$), C denotes the position of a fermion field component within a specific hypercube ($C_\mu \in \{0, 1\}$)] and $\gamma_C = \gamma_1^{C_1} \gamma_2^{C_2} \gamma_3^{C_3} \gamma_4^{C_4}$. In order to ensure the gauge invariance of the above operators, one inserts the quantity $U_{C,D}$, which is the average of products of gauge link variables along all possible shortest paths connecting the sites $y + C$ and $y + D$. In this work we focus on taste-singlet operators, thus $\xi = \mathbf{1}$. Explicitly, the taste-singlet bilinear operators can be written as:

$$\mathcal{O}_S(y) = \sum_D \bar{\chi}(y)_D \chi(y)_D \quad (13)$$

$$\mathcal{O}_V(y) = \sum_D \bar{\chi}(y)_{D+_2\hat{\mu}} U_{D+_2\hat{\mu},D} \chi(y)_D \eta_\mu(D) \quad (14)$$

$$\mathcal{O}_T(y) = \frac{1}{i} \sum_D \bar{\chi}(y)_{D+_2\hat{\mu}+_2\hat{\nu}} U_{D+_2\hat{\mu}+_2\hat{\nu},D} \chi(y)_D \eta_\nu(D) \eta_\mu(D+_2\hat{\nu}), \quad \mu \neq \nu \quad (15)$$

$$\mathcal{O}_A(y) = \sum_D \bar{\chi}(y)_{D+_2\hat{\mu}+_2(1,1,1,1)} U_{D+_2\hat{\mu}+_2(1,1,1,1),D} \chi(y)_D \eta_\mu(D) \cdot \eta_1(D+_2\hat{\mu}) \eta_2(D+_2\hat{\mu}) \eta_3(D+_2\hat{\mu}) \eta_4(D+_2\hat{\mu}) \quad (16)$$

$$\mathcal{O}_P(y) = \sum_D \bar{\chi}(y)_{D+_2(1,1,1,1)} U_{D+_2(1,1,1,1),D} \chi(y)_D \eta_1(D) \eta_2(D) \eta_3(D) \eta_4(D) \quad (17)$$

where S (Scalar), P (Pseudoscalar), V (Vector), A (Axial Vector), T (Tensor) correspond to: $\Gamma = \mathbf{1}, \gamma_5, \gamma_\mu, \gamma_5 \gamma_\mu, \gamma_5 \sigma_{\mu\nu}$ and $a+_2 b \equiv (a+b) \bmod 2$. Further details on the formulation of these operators are provided in Appendix A. With

the exception of the Scalar operator, the remaining operators contain averages of products of up to 4 gluon links (in orthogonal directions) between the fermion and the antifermion fields. Just as in the staggered fermion action, the gluon links used in the operators, are doubly stout links. We have kept the stout parameters of the action ($\omega_{A_1}, \omega_{A_2}$) distinct from the stout parameters of the operators ($\omega_{O_1}, \omega_{O_2}$), for wider applicability of the results. The presence of gluon links in the definition of bilinear operators creates new Feynman diagrams which do not appear in the Wilson formulation, leading to nontrivial contributions in our two-loop calculation.

C. Renormalization of fermion bilinear operators

The renormalization functions Z_Γ for lattice fermion bilinear operators, relate the bare operators $\mathcal{O}_{\Gamma_0} = \bar{\psi}\Gamma\psi$ to their corresponding renormalized continuum operators \mathcal{O}_Γ via:

$$\mathcal{O}_\Gamma = Z_\Gamma \mathcal{O}_{\Gamma_0} \quad (18)$$

Renormalization functions of such lattice operators are necessary ingredients in the prediction of physical probability amplitudes from lattice matrix elements. In order to calculate the renormalization functions Z_Γ , it is essential to compute the 2-point amputated Green's functions of the operators \mathcal{O}_{Γ_0} ; they can be written in the following form:

$$\Sigma_S(aq) = \mathbb{1} \Sigma_S^{(1)}(aq) \quad (19)$$

$$\Sigma_P(aq) = \gamma_5 \Sigma_P^{(1)}(aq) \quad (20)$$

$$\Sigma_V(aq) = \gamma_\mu \Sigma_V^{(1)}(aq) + \frac{q^\mu \not{q}}{q^2} \Sigma_V^{(2)}(aq) \quad (21)$$

$$\Sigma_A(aq) = \gamma_5 \gamma_\mu \Sigma_A^{(1)}(aq) + \gamma_5 \frac{q^\mu \not{q}}{q^2} \Sigma_A^{(2)}(aq) \quad (22)$$

$$\Sigma_T(aq) = \gamma_5 \sigma_{\mu\nu} \Sigma_T^{(1)}(aq) + \gamma_5 \frac{\not{q}}{q^2} (\gamma_\mu q_\nu - \gamma_\nu q_\mu) \Sigma_T^{(2)}(aq) \quad (23)$$

where $\Sigma_\Gamma^{(1)} = 1 + \mathcal{O}(g_\circ^2)$, $\Sigma_\Gamma^{(2)} = \mathcal{O}(g_\circ^2)$, g_\circ : bare coupling constant.

The RI' renormalization scheme is defined by imposing renormalization conditions on matrix elements at a scale $\bar{\mu}$. The renormalization condition giving $Z_\Gamma^{L,RI'}$ (L: Lattice) is:

$$\lim_{a \rightarrow 0} \left[Z_\psi^{L,RI'} Z_\Gamma^{L,RI'} \Sigma_\Gamma^{(1)}(aq) \right]_{\substack{q^2 = \bar{\mu}^2 \\ m=0}} = 1 \quad (24)$$

where Z_ψ is the renormalization function for the fermion field ($\psi = Z_\psi^{-1/2} \psi_\circ$, $\psi(\psi_\circ)$: renormalized (bare) fermion field). Such a condition guarantees that the renormalized Green's function of \mathcal{O}_Γ (the quantity in brackets in Eq. 24) will be a finite function of the renormalized coupling constant g for all values of the momenta ($g = \mu^{-\epsilon} Z_g^{-1} g_\circ$ where μ is the mass scale introduced to ensure that g_\circ has the correct dimensionality in $d = 4 - 2\epsilon$ dimensions). Comparison between the RI' and the $\overline{\text{MS}}$ schemes is normally performed at the same scale $\bar{\mu} = \mu(4\pi/e^{\gamma_E})^{1/2}$.

The RI' renormalization prescription, as given above, does not involve $\Sigma_\Gamma^{(2)}$; nevertheless, renormalizability of the theory implies that $Z_\Gamma^{L,RI'}$ will render the entire Green's function finite. An alternative prescription, more appropriate for nonperturbative renormalization, is:

$$\lim_{a \rightarrow 0} \left[Z_\psi^{L,RI'} Z_\Gamma^{L,RI'(\text{alter})} \frac{\text{tr}(\Gamma \Sigma_\Gamma(aq))}{\text{tr}(\Gamma \Gamma)} \right]_{\substack{q^2 = \bar{\mu}^2 \\ m=0}} = 1 \quad (25)$$

where a summation over repeated indices μ and ν is understood. This scheme has the advantage of taking into account the whole bare Green's function and therefore is useful for numerical simulations where the arithmetic data for Σ_Γ cannot be separated into two different structures. The two prescriptions differ between themselves (for V, A, T) by a finite amount which can be deduced from lower loop calculations combined with continuum results.

Conversion of renormalization functions from RI' to the \overline{MS} scheme is facilitated by the fact that renormalized Green's functions are regularization independent; thus the finite conversion factors:

$$C_\Gamma(g, \alpha) \equiv \frac{Z_\Gamma^{L, RI'}}{Z_\Gamma^{L, \overline{MS}}} = \frac{Z_\Gamma^{DR, RI'}}{Z_\Gamma^{DR, \overline{MS}}} \quad (26)$$

(DR: Dimensional Regularization, α : gauge parameter) can be evaluated in DR, leading to $Z_\Gamma^{L, \overline{MS}} = Z_\Gamma^{L, RI'} / C_\Gamma(g, \alpha)$. For the Pseudoscalar and Axial Vector operators, in order to satisfy Ward identities, additional finite factors $Z_5^P(g)$ and $Z_5^A(g)$, calculable in DR, are required:

$$Z_P^{L, \overline{MS}} = \frac{Z_P^{L, RI'}}{C_S Z_5^P}, \quad Z_A^{L, \overline{MS}} = \frac{Z_A^{L, RI'}}{C_V Z_5^A} \quad (27)$$

These factors are gauge independent; we also note that the value of Z_5^A for the flavor singlet operator differs from that of the nonsinglet one. The values of Z_5^P , $Z_5^{A(\text{singlet})}$ and $Z_5^{A(\text{nonsinglet})}$, calculated in Ref. [14], are:

$$Z_5^P(g) = 1 - \frac{g^2}{(4\pi)^2} (8c_F) + \frac{g^4}{(4\pi)^4} \left(\frac{2}{9} c_F N_c + \frac{4}{9} c_F N_f \right) + \mathcal{O}(g^6) \quad (28)$$

$$Z_5^{A(\text{singlet})}(g) = 1 - \frac{g^2}{(4\pi)^2} (4c_F) + \frac{g^4}{(4\pi)^4} \left(22c_F^2 - \frac{107}{9} c_F N_c + \frac{31}{18} c_F N_f \right) + \mathcal{O}(g^6) \quad (29)$$

$$Z_5^{A(\text{nonsinglet})}(g) = 1 - \frac{g^2}{(4\pi)^2} (4c_F) + \frac{g^4}{(4\pi)^4} \left(22c_F^2 - \frac{107}{9} c_F N_c + \frac{2}{9} c_F N_f \right) + \mathcal{O}(g^6) \quad (30)$$

where $c_F \equiv (N_c^2 - 1)/(2N_c)$ and N_f is the number of flavors.

III. COMPUTATION AND RESULTS

In the previous Section, the calculation setup was presented in rather general terms. Here we focus on the two-loop difference between flavor singlet and nonsinglet operator renormalization. Given that this difference first arises at two loops, we only need the tree-level values of Z_ψ , Z_g and of the conversion factors C_Γ , Z_5^P and Z_5^A ($Z_\psi = Z_g = C_\Gamma = Z_5^P = Z_5^A = 1$). Since $C_\Gamma = 1$, the difference up to two loops will not depend on the renormalization scheme. In addition, for our computations we will use mass-independent renormalization schemes; this means that the renormalized mass of quarks will be taken to be zero. For Wilson fermions, a zero renormalized mass entails a nonzero, $\mathcal{O}(g_s^2)$ Lagrangian mass; however, such a term does not enter the quantities which we calculate up to $\mathcal{O}(g_s^4)$.

A. Results from the Wilson formulation of the fermion action

At first, we present the computational procedure and results for the above difference using the Wilson formulation of the fermion action (Eq. 1). There are 5 two-loop Feynman diagrams contributing to this difference in the evaluation of the Green's functions (Eqs. 19 - 23), shown in Fig. 2. They all contain an operator insertion inside a closed fermion loop, and therefore vanish in the flavor nonsinglet case. Note that only diagrams 4 and 5 appear in the continuum. In order to simplify our calculations of Z_Γ , we worked with $\sum_x \mathcal{O}_\Gamma(x)$ so that no momentum enters the diagrams at

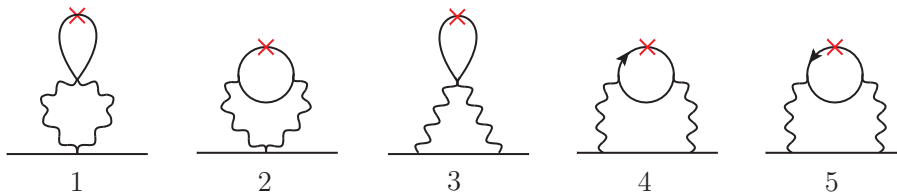


FIG. 2: Diagrams (in Wilson formulation) contributing to the difference between flavor singlet and nonsinglet values of Z_Γ . Solid (wavy) lines represent fermions (gluons). A cross denotes insertion of the operator \mathcal{O}_Γ .

the operator insertion point.

The above diagrams, evaluated individually, may be IR divergent, due to the presence of two-gluon propagators with the same momentum. Comparing to our previous evaluation of these diagrams with Wilson gluons and clover fermions [3, 4], we will find neither any new superficial divergences ($\ln^2(a^2\bar{\mu}^2)$ terms) nor any new subdivergences ($\ln(a^2\bar{\mu}^2)$ terms). However, the presence of stout links and Symanzik gluons leads to considerably longer expressions for the vertices. Also, the gluon propagator must now be inverted numerically for every choice of values for the Symanzik coefficients and for each value of the loop momentum 4-vector; an inversion in closed form exists, but it is not efficient.

The contribution of these diagrams to Z_P , Z_V , Z_T vanishes identically just as in continuum regularizations. Therefore, only Z_S and Z_A are affected. For the Scalar operator, our result can be written in the following form:

$$\begin{aligned}
Z_S^{\text{singlet}}(a\bar{\mu}) - Z_S^{\text{nonsinglet}}(a\bar{\mu}) = & \\
& - \frac{g_o^4}{(4\pi)^4} c_F N_f \left\{ (s_{00} + s_{01} \mathbf{csw} + s_{02} \mathbf{c}_{\text{SW}}^2 + s_{03} \mathbf{c}_{\text{SW}}^3 + s_{04} \mathbf{c}_{\text{SW}}^4) \right. \\
& + (s_{10} + s_{11} \mathbf{csw} + s_{12} \mathbf{c}_{\text{SW}}^2 + s_{13} \mathbf{c}_{\text{SW}}^3) \boldsymbol{\omega} + (s_{20} + s_{21} \mathbf{csw} + s_{22} \mathbf{c}_{\text{SW}}^2) \boldsymbol{\omega}^2 \\
& \left. + (s_{30} + s_{31} \mathbf{csw}) \boldsymbol{\omega}^3 + s_{40} \boldsymbol{\omega}^4 \right\} + \mathcal{O}(g_o^6) \tag{31}
\end{aligned}$$

The numerical constants s_{ij} have been computed for various sets of values of the Symanzik coefficients; their values are listed in Table II for the Wilson, TL Symanzik and Iwasaki gluon actions. The errors quoted stem from extrapolation of the results of numerical integration over loop momenta for different lattice sizes. The extrapolation methods that we used are described in Ref. [15]. The computation was performed in a general covariant gauge, confirming that the result is gauge independent, as it should be in \overline{MS} . We note from Eq. (31) that even single logarithms are absent, and thus the result is scale independent; this is consistent with the fact that the corresponding difference for the Scalar operator in dimensional regularization is absent.

	Wilson	TL Symanzik	Iwasaki		Wilson	TL Symanzik	Iwasaki
s_{00}	107.76(2)	76.29(1)	42.973(7)	a_{00}	2.051(2)	3.098(3)	5.226(4)
s_{01}	-82.27(1)	-69.01(1)	-49.356(8)	a_{01}	-15.033(3)	-12.851(3)	-9.426(3)
s_{02}	29.730(2)	26.178(1)	20.312(3)	a_{02}	-5.013(2)	-3.361(1)	-1.3526(7)
s_{03}	-3.4399(7)	-2.9533(5)	-2.2166(3)	a_{03}	2.1103(3)	1.7260(1)	1.1251(2)
s_{04}	-2.2750(4)	-1.6403(3)	-0.8547(2)	a_{04}	0.0434(2)	0.01636(1)	-0.01074(5)
s_{10}	-1854.4(2)	-1107.0(1)	-444.69(4)	a_{10}	43.75(1)	36.66(1)	25.827(9)
s_{11}	506.26(5)	364.01(3)	192.35(1)	a_{11}	76.993(3)	57.190(3)	31.768(2)
s_{12}	-95.42(2)	-70.94(1)	-40.162(6)	a_{12}	44.260(4)	29.363(2)	12.962(1)
s_{13}	7.494(1)	5.356(1)	2.8030(4)	a_{13}	-4.4660(6)	-3.3740(5)	-1.8710(2)
s_{20}	18317(2)	10081(1)	3511.3(4)	a_{20}	-126.45(1)	-92.853(7)	-50.378(1)
s_{21}	-2061.8(2)	-1350.7(1)	-595.79(7)	a_{21}	-259.59(3)	-175.65(2)	-81.45(1)
s_{22}	202.75(7)	133.19(4)	59.25(2)	a_{22}	-107.48(1)	-67.737(8)	-27.500(3)
s_{30}	-96390(10)	-50300(5)	-16185(2)	a_{30}	295.76(3)	198.78(2)	90.96(1)
s_{31}	3784.8(4)	2336.0(3)	925.6(1)	a_{31}	400.05(5)	253.87(3)	104.74(1)
s_{40}	213470(20)	106940(10)	32572(3)	a_{40}	-348.41(4)	-220.12(3)	-90.11(1)

TABLE II: Numerical coefficients for the Scalar and Axial Vector operators using Wilson/clover fermions.

For the Axial Vector operator we find:

$$\begin{aligned}
Z_A^{\text{singlet}}(a\bar{\mu}) - Z_A^{\text{nonsinglet}}(a\bar{\mu}) = & \\
& - \frac{g_o^4}{(4\pi)^4} c_F N_f \left\{ 6 \ln(a^2 \bar{\mu}^2) + (a_{00} + a_{01} \text{csw} + a_{02} \text{c}_{\text{SW}}^2 + a_{03} \text{c}_{\text{SW}}^3 + a_{04} \text{c}_{\text{SW}}^4) \right. \\
& + (a_{10} + a_{11} \text{csw} + a_{12} \text{c}_{\text{SW}}^2 + a_{13} \text{c}_{\text{SW}}^3) \omega + (a_{20} + a_{21} \text{csw} + a_{22} \text{c}_{\text{SW}}^2) \omega^2 \\
& \left. + (a_{30} + a_{31} \text{csw}) \omega^3 + a_{40} \omega^4 \right\} + \mathcal{O}(g_o^6) \tag{32}
\end{aligned}$$

By analogy with the scalar case, the computation was performed in a general gauge and the numerical constants a_{ij} are tabulated in Table II. We note that the result for the Axial Vector operator has a scale dependence; this is related to the axial anomaly.

Finally, the presence of a term of the form $\gamma_5 q_\mu q/q^2$ in the Green's function of the Axial Vector operator (Eq. 22) implies that, in the alternative RI' scheme mentioned in Section II C, the above result is modified by a finite term, as below:

$$Z_A^{\text{singlet}(\text{alter})}(a\bar{\mu}) - Z_A^{\text{nonsinglet}(\text{alter})}(a\bar{\mu}) = Z_A^{\text{singlet}}(a\bar{\mu}) - Z_A^{\text{nonsinglet}}(a\bar{\mu}) + \frac{g_o^4}{(4\pi)^4} c_F N_f \tag{33}$$

B. Results from the staggered formulation of the fermion action

In this subsection, we present the computational procedure and results using the staggered formulation of the fermion action (Eq. 6). In this case, there are some additional vertices with gluon lines stemming from the definition of bilinear operators (from the product $U_{C,D}$ in Eq. 11). As a result, there are 5 more Feynman diagrams, besides the 5 diagrams in Fig. 2, that enter our two-loop calculation. The extra diagrams involve operator vertices (the cross in the diagram) with up to two gluons. Fig. 3, shows a total of 10 two-loop Feynman diagrams contributing to the difference between singlet and nonsinglet Green's functions (Eqs. 19 - 23). For \mathcal{O}_S only diagrams 1, 2, 5, 6 and 7 contribute, since $U_{C,D} = 1$. Similarly to the case of Wilson fermions, we have worked with $\sum_y \mathcal{O}_\Gamma(y)$.

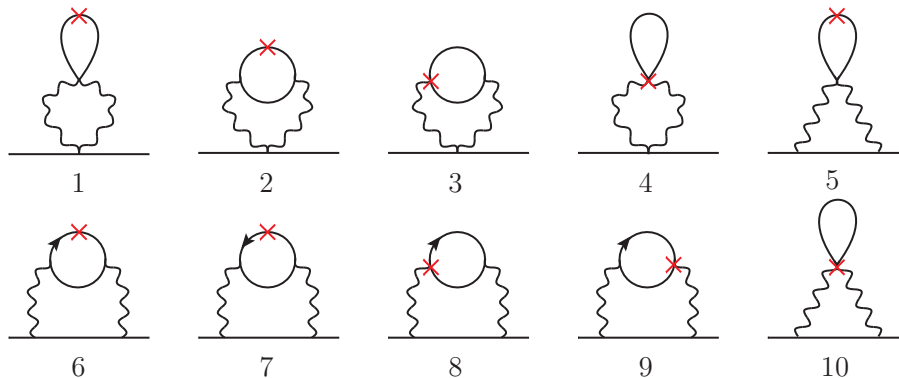


FIG. 3: Diagrams (in staggered formulation) contributing to the difference between flavor singlet and nonsinglet values of Z_Γ . Solid (wavy) lines represent fermions (gluons). A cross denotes insertion of the operator \mathcal{O}_Γ .

The above diagrams are more complicated than the corresponding diagrams in the Wilson case. One reason for this is the appearance of divergences in nontrivial corners of the Brillouin zone. Also, the presence of operator vertices with gluon lines, besides increasing the number of diagrams, gives terms with unusual offsets in momentum conservation delta functions (e.g., $\delta_{2\pi}^{(4)}(p_1 + p_2 + \pi\hat{\mu})$); it turns out that these terms vanish in the final expression of each diagram. In addition, the two (rather than one) smearing steps of gluon links in the fermion action, as well as in the operators, lead to extremely lengthy vertices; the lengthiest cases which appeared in our computation are the operator vertices with two gluons (~ 800000 terms for the Axial Vector). Since these vertices appear only with their fermion lines

contracted among themselves (diagrams: 4 and 10), we do not need to compute them as individual objects; we have used this fact in order to simplify the expression for diagrams 4 and 10.

Another important issue for the above diagrams is exploiting the underlying symmetries. For example in the Wilson case, the denominator of the fermion propagator satisfies the symmetry $p_\mu \rightarrow -p_\mu, \forall \mu$; in the staggered case there is another symmetry: $p_\mu \rightarrow p_\mu + \pi \hat{\nu}$, where μ, ν can be in the same or in different directions. This is a consequence of the semi-periodicity of the function $\sin^2(p_\mu)$, which appears in the denominator of the staggered propagator (rather than $\sin^2(p_\mu/2)$). These symmetries help us to reduce the number of terms in the diagrams, eliminating odd integrands.

As in the Wilson case, the contribution of the diagrams in Fig. 3 to Z_P, Z_V, Z_T vanishes. Furthermore, in contrast to the Wilson case, Z_S also receives a vanishing contribution. The closed fermion loop of the diagrams which contribute to Z_S, Z_P, Z_T , gives an odd number of exponentials of the inner momentum; this leads to odd integrands, which equal zero, due to the symmetry of the staggered propagator mentioned above. So, for the cases of Z_S, Z_P, Z_T , the contribution vanishes diagram by diagram. Conversely, for the case of Z_V , each diagram vanishes when we add its symmetric diagram (diagrams 6+7, 8+9). Therefore, only Z_A is affected. In particular, only diagrams 6 - 9 contribute to Z_A ; the remaining diagrams vanish. Then, for the Axial Vector operator, our result can be written in the following form:

$$\begin{aligned}
Z_A^{\text{singlet}}(a\bar{\mu}) - Z_A^{\text{nonsinglet}}(a\bar{\mu}) = & \\
& - \frac{g_o^4}{(4\pi)^4} c_F N_f \left\{ 6 \ln(a^2 \bar{\mu}^2) + \alpha_1 + \alpha_2 (\omega_{A_1} + \omega_{A_2}) + \alpha_3 (\omega_{A_1}^2 + \omega_{A_2}^2) + \alpha_4 \omega_{A_1} \omega_{A_2} \right. \\
& + \alpha_5 (\omega_{A_1}^3 + \omega_{A_2}^3) + \alpha_6 \omega_{A_1} \omega_{A_2} (\omega_{A_1} + \omega_{A_2}) + \alpha_7 (\omega_{A_1}^4 + \omega_{A_2}^4) + \alpha_8 \omega_{A_1}^2 \omega_{A_2}^2 \\
& + \alpha_9 \omega_{A_1} \omega_{A_2} (\omega_{A_1}^2 + \omega_{A_2}^2) + \alpha_{10} \omega_{A_1}^2 \omega_{A_2}^2 (\omega_{A_1} + \omega_{A_2}) + \alpha_{11} \omega_{A_1} \omega_{A_2} (\omega_{A_1}^3 + \omega_{A_2}^3) \\
& + \alpha_{12} \omega_{A_1}^3 \omega_{A_2}^3 + \alpha_{13} \omega_{A_1}^2 \omega_{A_2}^2 (\omega_{A_1}^2 + \omega_{A_2}^2) + \alpha_{14} \omega_{A_1}^3 \omega_{A_2}^3 (\omega_{A_1} + \omega_{A_2}) \\
& + \alpha_{15} \omega_{A_1}^4 \omega_{A_2}^4 + \alpha_{16} (\omega_{O_1} + \omega_{O_2}) + \alpha_{17} \omega_{O_1} \omega_{O_2} + \alpha_{18} (\omega_{A_1} + \omega_{A_2}) (\omega_{O_1} + \omega_{O_2}) \\
& + \alpha_{19} \omega_{A_1} \omega_{A_2} (\omega_{O_1} + \omega_{O_2}) + \alpha_{20} \left[(\omega_{A_1}^2 + \omega_{A_2}^2) (\omega_{O_1} + \omega_{O_2}) + (\omega_{A_1} + \omega_{A_2}) \omega_{O_1} \omega_{O_2} \right] \\
& + \alpha_{21} (\omega_{A_1}^2 + \omega_{A_2}^2) \omega_{O_1} \omega_{O_2} + \alpha_{22} (\omega_{A_1}^3 + \omega_{A_2}^3) (\omega_{O_1} + \omega_{O_2}) \\
& + \alpha_{23} \omega_{A_1} \omega_{A_2} \left[(\omega_{A_1} + \omega_{A_2}) (\omega_{O_1} + \omega_{O_2}) + \omega_{O_1} \omega_{O_2} \right] + \alpha_{24} (\omega_{A_1}^3 + \omega_{A_2}^3) \omega_{O_1} \omega_{O_2} \\
& + \alpha_{25} \omega_{A_1} \omega_{A_2} (\omega_{A_1}^2 + \omega_{A_2}^2) (\omega_{O_1} + \omega_{O_2}) \\
& + \alpha_{26} \omega_{A_1} \omega_{A_2} \left[\omega_{A_1} \omega_{A_2} (\omega_{O_1} + \omega_{O_2}) + (\omega_{A_1} + \omega_{A_2}) \omega_{O_1} \omega_{O_2} \right] + \alpha_{27} \omega_{A_1}^2 \omega_{A_2}^2 \omega_{O_1} \omega_{O_2} \\
& + \alpha_{28} \omega_{A_1} \omega_{A_2} \left[\omega_{A_1} \omega_{A_2} (\omega_{A_1} + \omega_{A_2}) (\omega_{O_1} + \omega_{O_2}) + (\omega_{A_1}^2 + \omega_{A_2}^2) \omega_{O_1} \omega_{O_2} \right] \\
& + \alpha_{29} \omega_{A_1}^3 \omega_{A_2}^3 (\omega_{O_1} + \omega_{O_2}) + \alpha_{30} \omega_{A_1}^2 \omega_{A_2}^2 (\omega_{A_1} + \omega_{A_2}) \omega_{O_1} \omega_{O_2} \\
& \left. + \alpha_{31} \omega_{A_1}^3 \omega_{A_2}^3 \omega_{O_1} \omega_{O_2} \right\} + \mathcal{O}(g_o^6) \tag{34}
\end{aligned}$$

The computation was performed in a general gauge and the numerical constants α_i are tabulated in Table III. The computation with staggered fermions gives rise to some nontrivial divergent integrals, which cannot be present in the Wilson formulation due to the different pole structure of the fermion propagator. In Appendix B, we provide a brief description of the manipulations performed to evaluate such divergent terms. We note that the result for the Axial Vector operator, as we expected, has the same divergent behaviour just as in the Wilson case and in the continuum, i.e. $6 \ln(a^2 \bar{\mu}^2)$. As was expected, this logarithmic divergence originates in diagrams 6 and 7, which are the only ones present in the continuum. Also, in the alternative RI' scheme we must add the same finite term, $g_o^4/(4\pi)^4 c_F N_f$, as in the Wilson case.

	Wilson	TL Symanzik	Iwasaki		Wilson	TL Symanzik	Iwasaki
α_1	17.420(1)	16.000(1)	14.610(1)	α_{16}	24.9873(2)	18.0489(4)	9.9571(2)
α_2	-116.049(7)	-81.342(5)	-41.583(2)	α_{17}	-97.4550(2)	-62.2675(1)	-26.5359(1)
α_3	839.788(9)	539.121(6)	230.050(1)	α_{18}	-292.3650(5)	-186.8025(4)	-79.6078(2)
α_4	2175.14(3)	1394.12(2)	591.88(1)	α_{19}	4864.513(9)	2921.876(6)	1107.333(2)
α_5	-3462.830(1)	-2098.136(5)	-801.633(3)	α_{20}	1621.504(3)	973.959(2)	369.111(1)
α_6	-19565.9(1)	-11858.6(1)	-4528.6(1)	α_{21}	-10617.81(2)	-6122.11(1)	-2169.30(1)
α_7	6424.33(2)	3740.18(1)	1337.93(1)	α_{22}	-3539.269(6)	-2040.705(4)	-723.099(1)
α_8	200966.5(4)	117179.7(4)	41977.1(1)	α_{23}	-31853.42(5)	-18366.34(3)	-6507.89(1)
α_9	92171.5(3)	53720.8(1)	19237.6(1)	α_{24}	25847.14(3)	14435.59(2)	4881.52(1)
α_{10}	-1026448(1)	-580271(2)	-198722(1)	α_{25}	77541.41(1)	43306.78(6)	14644.54(2)
α_{11}	-183998.3(3)	-103929.7(3)	-35561.1(1)	α_{26}	232624.2(3)	129920.3(2)	43933.6(1)
α_{12}	5517230(30)	3037110(10)	1003641(1)	α_{27}	-1844375(1)	-1002465(1)	-326727(1)
α_{13}	2145810(10)	1180684(4)	389979(1)	α_{28}	-614791.6(6)	-334155.0(4)	-108909.0(2)
α_{14}	-11889300(40)	-6386950(30)	-2046240(10)	α_{29}	1736048.1(8)	920956.7(7)	290916.1(3)
α_{15}	26137700(200)	13729010(10)	4278680(10)	α_{30}	5208144(2)	2762870(2)	872748(1)
				α_{31}	-15545543(1)	-8065557(2)	-2478207(1)

TABLE III: Numerical coefficients for the Axial Vector operator using staggered fermions.

IV. DISCUSSION

The numerical value of the difference between singlet and nonsinglet renormalization functions can be very significant, depending on the values of the parameters employed in the action. In order to assess the importance of this difference, we present here several graphs of the results for certain values of c_i , c_{SW} and ω for the Wilson case and c_i , ω_{A_1} , ω_{A_2} , ω_{O_1} and ω_{O_2} for the staggered case.

In Figs. (4 - 5) we illustrate our results from the Wilson formulation by selecting values for parameters c_{SW} and ω . We compute the contribution to ζ , defined through:

$$Z_{\Gamma}^{(\text{singlet})} - Z_{\Gamma}^{(\text{nonsinglet})} = \frac{g_o^4}{(4\pi)^4} N_f c_F \zeta \quad (35)$$

using different gluon actions: Wilson, tree-level Symanzik, Iwasaki, DBW2. We notice that the Iwasaki and DBW2 actions exhibit a milder dependence altogether on c_{SW} and ω . Certain values of c_{SW} and ω lead to almost vanishing contributions to ζ in the Scalar case (and less so in the Axial Vector case) for all gluon actions considered (see right panels of Fig. 4).

In Fig. 6 we have selected parameter values appropriate to the ETMC action with Iwasaki gluons, $N_f = 2 + 1 + 1$, $\beta = 2N_c/g_o^2 = 1.95$, $\bar{\mu} = 1/a$ and standard/stout links for the Wilson part of the fermion action. Results from this work have been successfully applied by the ETM Collaboration for the renormalization of the individual quark contributions to the intrinsic spin [16]. We anticipate further use of our results for other action parameters in the near future. Fig. 7 presents our results for parameter values appropriate to the SLiNC action, with tree-level Symanzik gluons, $N_f = 3$, $\beta = 2N_c c_0/g_o^2 = 5.5$, $\bar{\mu} = 1/a$.

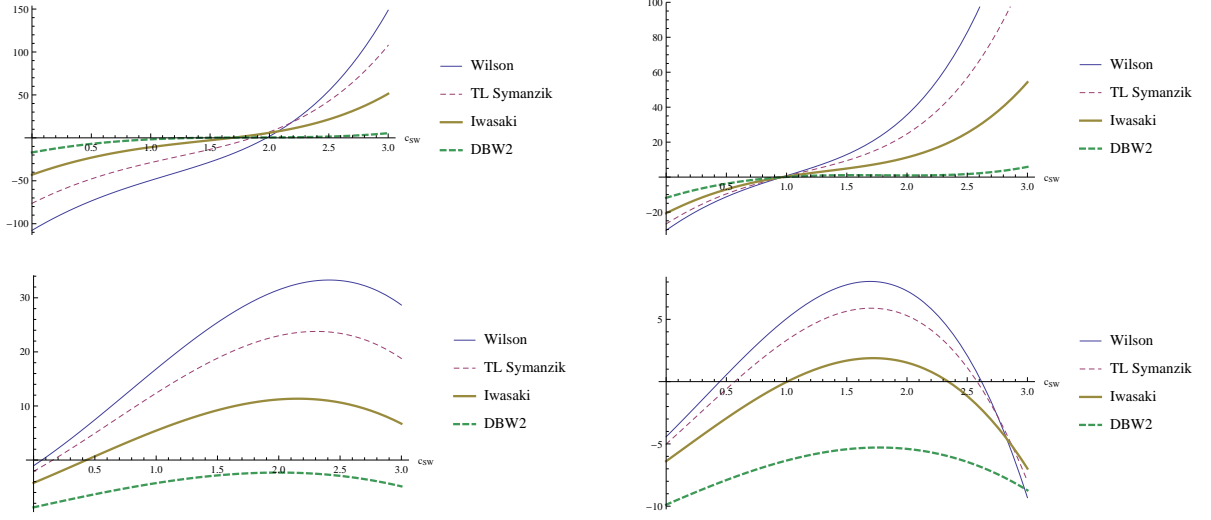


FIG. 4: Plots of $\zeta \equiv [Z_{\Gamma}^{(\text{singlet})} - Z_{\Gamma}^{(\text{nonsinglet})}] \left(\frac{g_{\alpha}^4}{(4\pi)^4} N_f c_F \right)^{-1}$, for Scalar $\Gamma = S$ (top panels) and Axial Vector $\Gamma = A$ (bottom panels), as a function of c_{SW} , for $\omega = 0$ (left panels) and $\omega = 0.1$ (right panels).

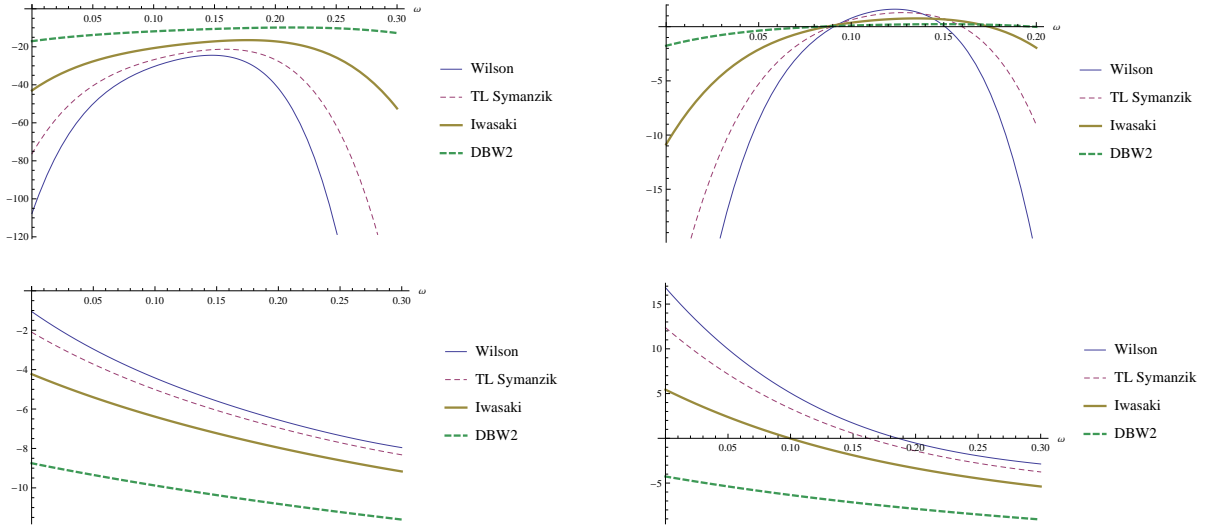


FIG. 5: Plots of $\zeta \equiv [Z_{\Gamma}^{(\text{singlet})} - Z_{\Gamma}^{(\text{nonsinglet})}] \left(\frac{g_{\alpha}^4}{(4\pi)^4} N_f c_F \right)^{-1}$, for Scalar $\Gamma = S$ (top panels) and Axial Vector $\Gamma = A$ (bottom panels), as a function of ω , for $c_{SW} = 0$ (left panels) and $c_{SW} = 1$ (right panels).

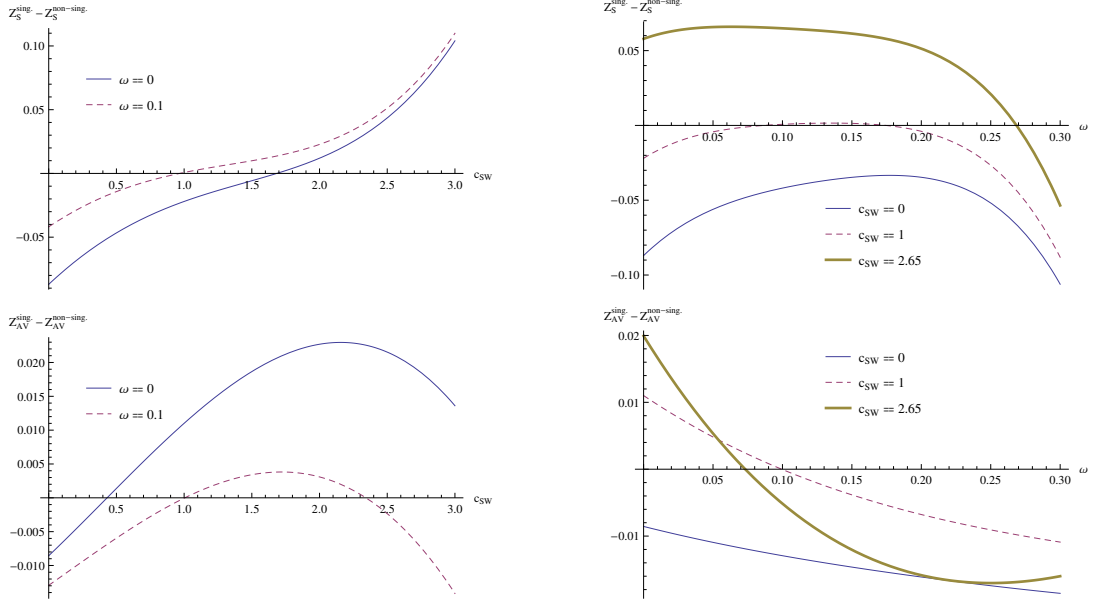


FIG. 6: Plots of $Z_{\Gamma}^{\text{singlet}} - Z_{\Gamma}^{\text{non-singlet}}$, for Scalar $\Gamma = S$ (top panels) and Axial Vector $\Gamma = AV$ (bottom), as a function of c_{SW} (left) and ω (right). Parameter values relevant for ETMC action ($N_f = 4$, Iwasaki gluons, $\beta = 1.95$).

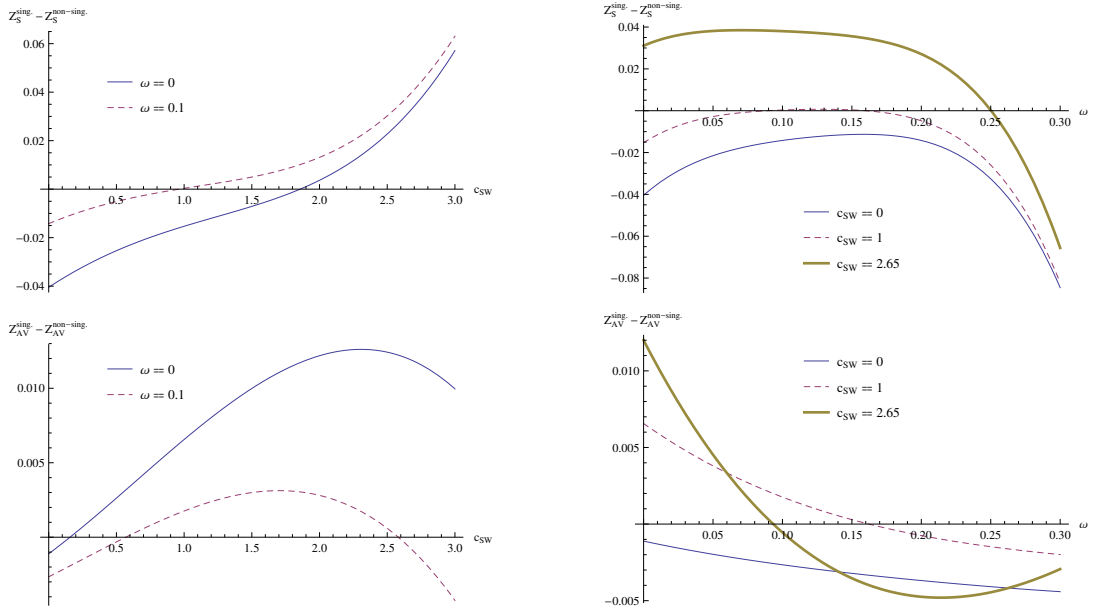


FIG. 7: Plots of $Z_{\Gamma}^{\text{singlet}} - Z_{\Gamma}^{\text{non-singlet}}$, for Scalar $\Gamma = S$ (top panels) and Axial Vector $\Gamma = AV$ (bottom), as a function of c_{SW} (left) and ω (right). Parameter values relevant for SLiNC action ($N_f = 3$, TL Symanzik gluons, $\beta = 5.5$).

In the staggered formulation, we note that the result (34) is symmetric under the exchange of ω_{AS} as well as under the exchange of ω_{OS} . This fact is consistent with the requirement that the results for $(\omega_{O_1} = 0, \omega_{O_2} = \omega)$ and $(\omega_{O_1} = \omega, \omega_{O_2} = 0)$ should coincide, since they both correspond to a single smearing step; similarly for the coefficients ω_{A_1} and ω_{A_2} . These properties provide nontrivial consistency checks of our computation.

In Fig. 8 we present 2D graphs of our results by selecting the following parameter values:

1. $\omega_{A_1} = \omega_{A_2} = \omega_{O_1} = \omega_{O_2} = \omega$
2. $\omega_{A_1} = \omega_{A_2} = \omega, \omega_{O_1} = \omega_{O_2} = 0$ (No smearing procedure in the links of operators)
3. $\omega_{A_1} = \omega, \omega_{A_2} = \omega_{O_1} = \omega_{O_2} = 0$ (One smearing step only in the links of fermion action)
4. $\omega_{A_1} = \omega_{O_1} = \omega, \omega_{A_2} = \omega_{O_2} = 0$ (One smearing step in the links of fermion action and operators).

The vertical axis of these plots corresponds to $Z_A^{\text{diff.}} \equiv \left[Z_A^{(\text{singlet})}(a\bar{\mu}) - Z_A^{(\text{nonsinglet})}(a\bar{\mu}) \right] \left(-\frac{g_o^4}{(4\pi)^4} N_f c_F \right)^{-1}$ for $\bar{\mu} = 1/a$. We plot the results for gluon actions: Wilson, tree-level Symanzik, Iwasaki in the same graph. We notice that the plots for the Iwasaki action are flatter than for the remaining actions but the Wilson action has the smallest values of $Z_A^{\text{diff.}}$.

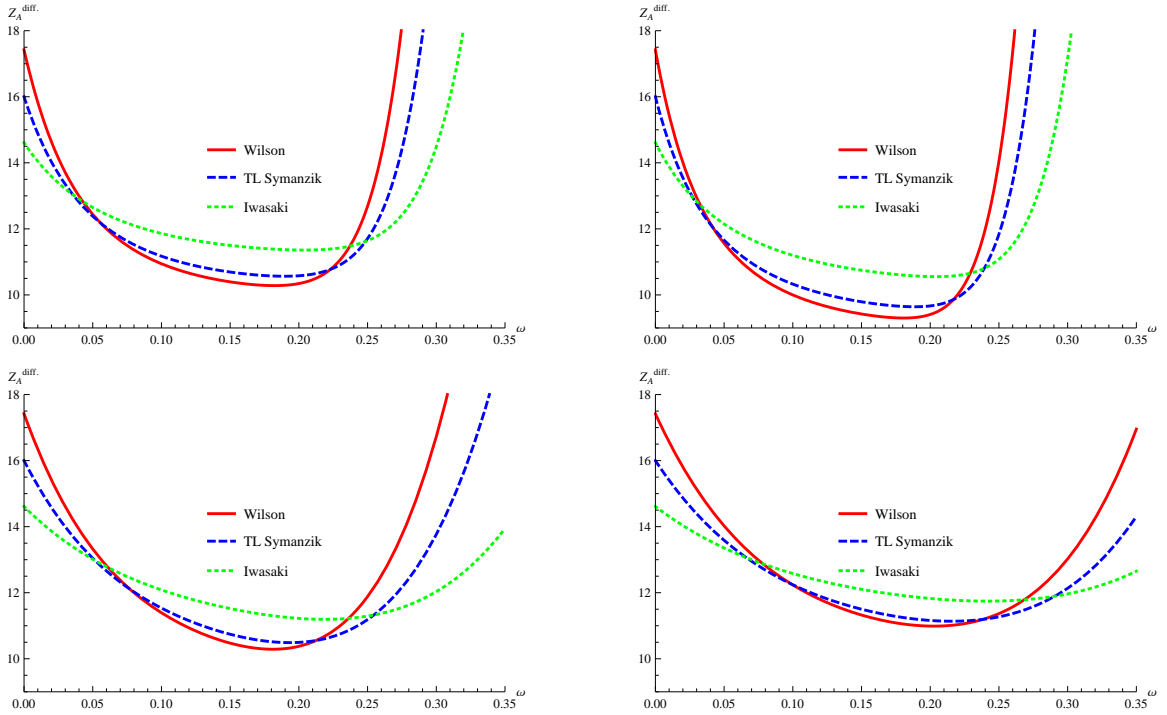


FIG. 8: Plots of $Z_A^{\text{diff.}} \equiv \left[Z_A^{(\text{singlet})} - Z_A^{(\text{nonsinglet})} \right] \left(-\frac{g_o^4}{(4\pi)^4} N_f c_F \right)^{-1}$, as a function of ω for the parameter values: upper left: $\omega_{A_1} = \omega_{A_2} = \omega_{O_1} = \omega_{O_2} = \omega$, upper right: $\omega_{A_1} = \omega_{A_2} = \omega, \omega_{O_1} = \omega_{O_2} = 0$, lower left: $\omega_{A_1} = \omega, \omega_{A_2} = \omega_{O_1} = \omega_{O_2} = 0$, lower right: $\omega_{A_1} = \omega_{O_1} = \omega, \omega_{A_2} = \omega_{O_2} = 0$.

In Figs. (9 - 11) we present 3D graphs of our results by selecting the following parameter values:

Fig. 9: $\omega_{A_1}, \omega_{A_2}$: free parameters and $\omega_{O_1} = \omega_{O_2} = 0$ (No smearing procedure in the links of operators)

Fig. 10: $\omega_{A_1}, \omega_{O_1}$: free parameters and $\omega_{A_2} = \omega_{O_2} = 0$ (One smearing step in the links of fermion action and operators)

Fig. 11: $\omega_{A_1} = \omega_{A_2}, \omega_{O_1} = \omega_{O_2}$.

Just as in 2D graphs, the vertical axis of these plots corresponds to $Z_A^{\text{diff.}}$ for $\bar{\mu} = 1/a$. We notice again that the plots for the Iwasaki action are flatter than the remaining actions. Also, from the first trio of graphs (Fig. 9), we notice that there is only one minimum, on the 45° axis. Therefore, the two smearing steps of the fermion action give better results than only one smearing step. Also, in Fig. 10, as well as in Fig. 11, we observe that the stout smearing of the action is more effective in minimizing $Z_A^{\text{diff.}}$ than the stout smearing of operators.

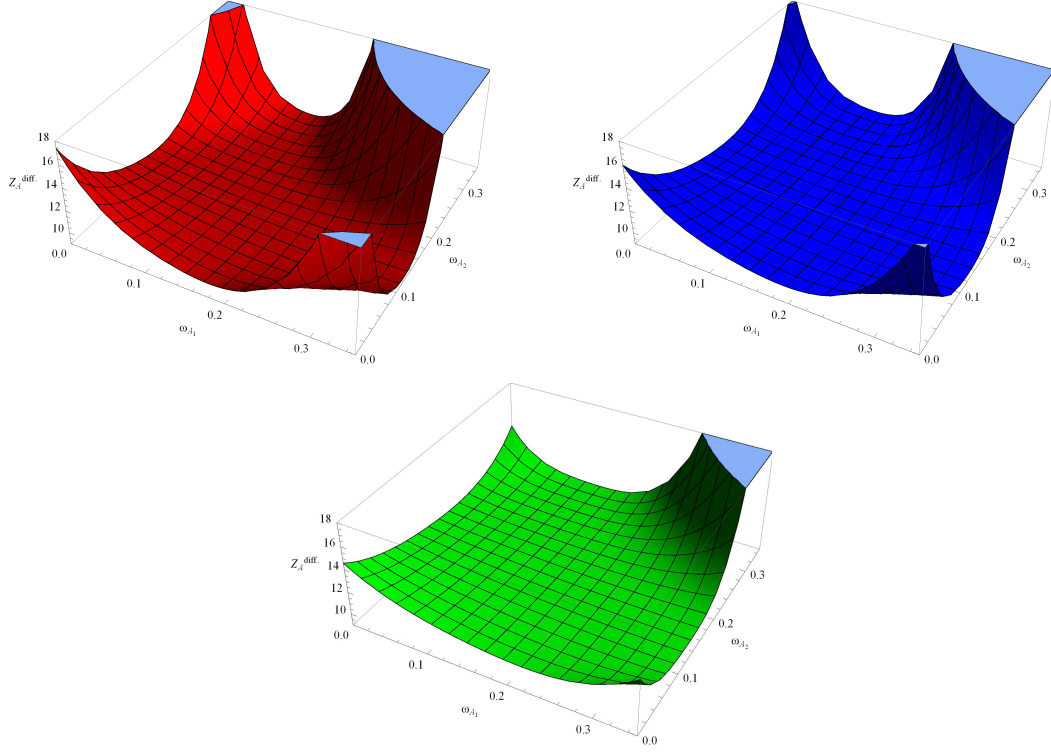


FIG. 9: Plots of $Z_A^{\text{diff.}} \equiv \left[Z_A^{(\text{singlet})} - Z_A^{(\text{nonsinglet})} \right] \left(-\frac{g_o^4}{(4\pi)^4} N_f C_F \right)^{-1}$, as a function of ω_{A1} and ω_{A2} for $\omega_{O1} = \omega_{O2} = 0$ (upper left: Wilson action, upper right: TL Symanzik action, lower: Iwasaki action).

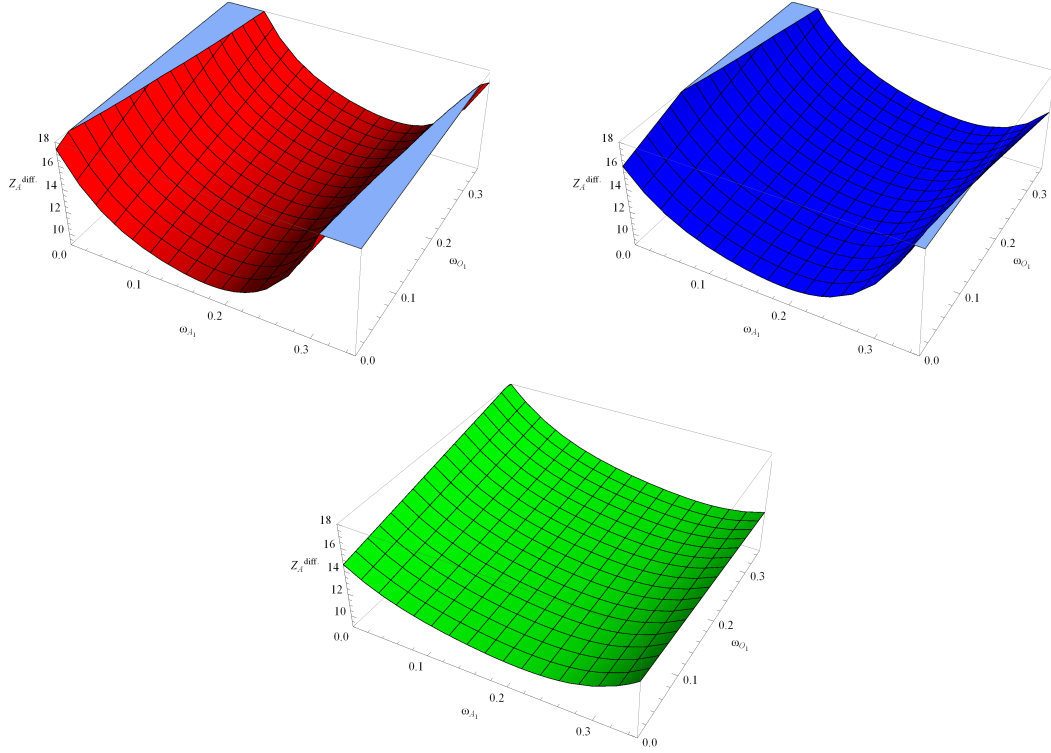


FIG. 10: Plots of $Z_A^{\text{diff.}} \equiv \left[Z_A^{(\text{singlet})} - Z_A^{(\text{nonsinglet})} \right] \left(-\frac{g_o^4}{(4\pi)^4} N_f C_F \right)^{-1}$, as a function of ω_{A1} and ω_{O1} for $\omega_{A2} = \omega_{O2} = 0$ (upper left: Wilson action, upper right: TL Symanzik action, lower: Iwasaki action).

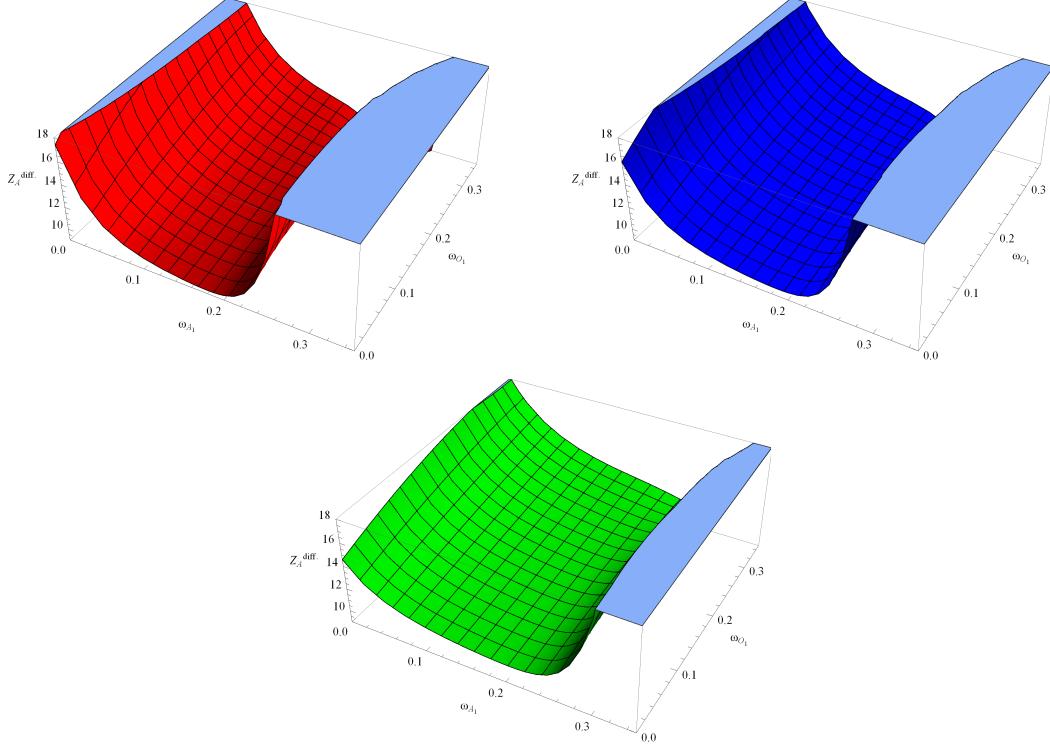


FIG. 11: Plots of $Z_A^{\text{diff.}} \equiv [Z_A^{(\text{singlet})} - Z_A^{(\text{nonsinglet})}] \left(-\frac{g_o^4}{(4\pi)^4} N_f c_F \right)^{-1}$, as a function of ω_{A_1} and ω_{O_1} for $\omega_{A_2} = \omega_{A_1}$ and $\omega_{O_2} = \omega_{O_1}$ (upper left: Wilson action, upper right: TL Symanzik action, lower: Iwasaki action).

Further extensions of the present work include the application to other actions currently used in numerical simulations, including actions with more steps of stout smearing. In these cases, additional contributions to the renormalization functions are more convergent, and thus their perturbative treatment is simpler; nevertheless, the sheer size of the vertices (already with 2 stout-smearing steps we have encountered $\sim 10^6$ terms) renders the computation quite cumbersome. Another possible extension of this work regards several variants of staggered fermion action (e.g., HYP smearing [17], HEX smearing [18], Asqtad [19]). Finally, extended versions of $\bar{\psi}\Gamma\psi$ may be studied; in this case the Feynman diagrams of the Fig. 3 will apply also to Wilson fermions and loop integrands will typically contain a plethora of new terms, which however will be convergent.

Appendix A: Fermion action and fermion bilinear operators in the staggered formulation

In this appendix we present the derivation of the staggered fermion action and the definition of fermion bilinear operators in the staggered formulation. We start from the naive fermion action:

$$S_F = a^4 \sum_{x, \mu} \bar{\psi}(x) (\gamma_\mu D_\mu) \psi(x) + a^4 \sum_x m \bar{\psi}(x) \psi(x) \quad (\text{A1})$$

where the covariant derivative D_μ is defined as follows:

$$D_\mu \psi(x) = \frac{1}{2a} \left[U_\mu(x) \psi(x + a\hat{\mu}) - U_\mu^\dagger(x - a\hat{\mu}) \psi(x - a\hat{\mu}) \right] \quad (\text{A2})$$

The above naive action presents the well-known doubling problem. The standard passage to the staggered action entails the following change of basis:

$$\begin{aligned} \psi(x) &= \gamma_x \chi(x) \quad , \quad \bar{\psi}(x) = \bar{\chi}(x) \gamma_x^\dagger, \\ \gamma_x &= \gamma_1^{n_1} \gamma_2^{n_2} \gamma_3^{n_3} \gamma_4^{n_4} \quad , \quad x = (a n_1, a n_2, a n_3, a n_4), \quad n_i \in \mathbb{Z} \end{aligned} \quad (\text{A3})$$

Using the equalities

$$\gamma_\mu \gamma_x = \eta_\mu(x) \gamma_{x+a\hat{\mu}} \quad \text{and} \quad \gamma_x^\dagger \gamma_x = \mathbf{1} \quad , \quad \eta_\mu(x) = (-1)^{\sum_{\nu < \mu} n_\nu} \quad (\text{A4})$$

the lattice fermion action takes the form:

$$S_F = a^4 \sum_x \sum_\mu \frac{1}{2a} \bar{\chi}(x) \eta_\mu(x) \left[U_\mu(x) \chi(x + a\hat{\mu}) - U_\mu^\dagger(x - a\hat{\mu}) \chi(x - a\hat{\mu}) \right] + a^4 \sum_x m \bar{\chi}(x) \chi(x) \quad (\text{A5})$$

The absence of Dirac indices in the action leads to the assigning of a single fermion field component to each lattice site. Hence, the action contains only four rather than sixteen fermion doublers, which are called ‘‘tastes’’.

In the staggered formalism a physical fermion field $\psi(x)$ with taste components is defined as a linear combination of the single-component fermion fields $\chi(x)$ that live on the corners of 4-dimensional elementary hypercubes of the lattice. In standard notation:

$$\psi_{\alpha,t}(y) = \frac{1}{2} \sum_C (\gamma_C)_{\alpha,t} \chi(y)_C \quad , \quad \chi(y)_C = \frac{1}{2} \sum_{\alpha,t} (\xi_C)_{\alpha,t} \psi_{\alpha,t}(y) \quad (\text{A6})$$

where $\chi(y)_C \equiv \chi(y+aC)/4$, y denotes the position of a hypercube inside the lattice ($y_\mu \in 2\mathbb{Z}$), C denotes the position of a fermion field component within a specific hypercube ($C_\mu \in \{0, 1\}$), $\gamma_C = \gamma_1^{C_1} \gamma_2^{C_2} \gamma_3^{C_3} \gamma_4^{C_4}$, $\xi_C = \xi_1^{C_1} \xi_2^{C_2} \xi_3^{C_3} \xi_4^{C_4}$, $\xi_\mu = \gamma_\mu^*$, α is a Dirac index and t is a taste index. In terms of fermion fields with taste components one can now define fermion bilinear operators as in Eq. (10): $\mathcal{O}_{\Gamma,\xi} = \bar{\psi}(x) (\Gamma \otimes \xi) \psi(x)$. Transforming to the staggered basis via Eq. (A6), we extract Eqs. (11 - 12). Using the relations $\gamma_\mu \gamma_C = \eta_\mu(C) \gamma_{C+\hat{\mu}}$ and $\text{tr}(\gamma_C^\dagger \gamma_D) = 4\delta_{C,D}$, we calculate the quantity $(\overline{\Gamma \otimes \mathbf{1}})_{CD}$ for each operator Γ :

$$\begin{aligned} \frac{1}{4} \text{Tr} \left[\gamma_C^\dagger \mathbf{1} \gamma_D \right] &= \delta_{C,D} \quad , \\ \frac{1}{4} \text{Tr} \left[\gamma_C^\dagger \gamma_\mu \gamma_D \right] &= \delta_{C,D+2\hat{\mu}} \eta_\mu(D) \quad , \\ \frac{1}{4} \text{Tr} \left[\gamma_C^\dagger \sigma_{\mu\nu} \gamma_D \right] &= \frac{1}{i} \delta_{C,D+2\hat{\mu}+2\hat{\nu}} \eta_\nu(D) \eta_\mu(D+2\hat{\nu}) \quad , \\ \frac{1}{4} \text{Tr} \left[\gamma_C^\dagger \gamma_5 \gamma_\mu \gamma_D \right] &= \delta_{C,D+2\hat{\mu}+2(1,1,1,1)} \eta_\mu(D) \eta_1(D+2\hat{\mu}) \eta_2(D+2\hat{\mu}) \eta_3(D+2\hat{\mu}) \eta_4(D+2\hat{\mu}) \quad , \\ \frac{1}{4} \text{Tr} \left[\gamma_C^\dagger \gamma_5 \gamma_D \right] &= \delta_{C,D+2(1,1,1,1)} \eta_1(D) \eta_2(D) \eta_3(D) \eta_4(D) \end{aligned} \quad (\text{A7})$$

where $a+2b \equiv (a+b) \bmod 2$. Now, the operators can be written as in Eqs. (13 - 17), where the Scalar, Vector, Tensor, Axial Vector and Pseudoscalar operators contain the average of products of 0, 1, 2, 3 and 4 gluon links, respectively. For example, the average entering the tensor operator of Eq. (16) is:

$$U_{D+2\hat{\mu}+2\hat{\nu},D} = \frac{1}{2} \left[U_\nu^\dagger(y+aD+2a\hat{\mu}) U_\mu^\dagger(y+aD) + \{\mu \leftrightarrow \nu\} \right] \quad (\text{A8})$$

(Eq. A8 is valid when $(D +_2 \hat{\mu} +_2 \hat{\nu})_i \geq D_i$, $i = 1, 2, 3, 4$, and takes a similar form for all other cases.)

Another aspect of the staggered formalism is the representation of the action as well as the representation of the bilinears in momentum space. In order to do this, we use some useful relations, such as the following equivalent expression of $\eta_\mu(x)$:

$$\eta_\mu(x) = e^{i\pi\bar{\mu}n}, \quad x = an, \quad \bar{\mu} = \sum_{\nu=1}^{\mu-1} \hat{\nu} \quad (\text{A9})$$

Also, the summation over the position of \mathcal{O}_Γ , followed by Fourier transformation leads to expressions of the form:

$$\sum_{y_\mu \in 2\mathbb{Z}} e^{iy \cdot k} = \frac{1}{16} (2\pi)^4 \sum_C \delta_{2\pi}^{(4)}(k + \pi C) \quad (\text{A10})$$

where $\delta_{2\pi}^{(4)}(k)$ stands for the standard periodic δ -function with nonvanishing support at $k \bmod 2\pi = 0$. In addition, the summation over the index D in the definition of \mathcal{O}_Γ , after Fourier transformation, may give expressions such as:

$$\sum_D e^{-i\pi(C-E) \cdot D} = 16 \delta_{C,E} \quad (\text{A11})$$

where $E = (E_1, E_2, E_3, E_4)$, $E_\mu \in \{0, 1\}$. Furthermore, expressions like $e^{ik(D+_2\hat{\mu})a}$ (for Vector and similar expressions for all other operators), which arise through Fourier transformations of the fermion and the antifermion fields, can be written in the following useful form:

$$e^{ik(D+_2\hat{\mu})a} = e^{ikDa} [\cos(k_\mu a) + ie^{i\pi D \cdot \hat{\mu}} \sin(k_\mu a)] \quad (\text{A12})$$

Finally, since contributions to the continuum limit come from the neighbourhood of each of the 16 poles of the external momenta q , at $q_\mu = (\pi/a)C_\mu$, it is useful to define q'_μ and C_μ through

$$q_\mu = q'_\mu + \frac{\pi}{a} C_\mu \pmod{\left(\frac{2\pi}{a}\right)}, \quad (C_\mu \in \{0, 1\}) \quad (\text{A13})$$

where the ‘‘small’’ (physical) part q' has each of its components restricted to one half of the Brillouin zone: $-\pi/(2a) \leq q'_\mu \leq \pi/(2a)$. Thus, conservation of external momenta takes the form:

$$\delta_{2\pi}^{(4)}(a q_1 - a q_2 + \pi D) = \frac{1}{a} \delta^{(4)}(q'_1 - q'_2) \prod_\mu \delta_{C_{1\mu+_2} C_{2\mu+_2} D_\mu, 0} \quad (\text{A14})$$

Appendix B: Evaluation of a basis of nontrivial divergent two-loop Feynman diagrams in the staggered formalism

In this appendix we present the procedure that we used to evaluate nontrivial divergent integrals which appeared in our two-loop computation using staggered fermions. In the Wilson case, the two-loop divergent integrals, which appeared, can be expressed in terms of a basis of standard integrals found in Ref. [20], along with manipulations found in Ref. [4]. However, in the staggered case, the divergent integrals are not related to those standard integrals in an obvious way. Some further steps are needed to this end.

In our computation, there appeared 4 types of nontrivial divergent 2-loop integrals, using staggered fermions; they are listed below:

$$I_{1\mu\nu} = \int_{-\pi}^{\pi} \frac{d^4k}{(2\pi)^4} \frac{\overset{\circ}{k}_\mu \overset{\circ}{k}_\nu}{(\widehat{k^2})^2 (\widehat{k+aq})^2} \int_{-\pi}^{\pi} \frac{d^4p}{(2\pi)^4} \frac{1}{\overset{\circ}{p}^2 (\overset{\circ}{p+k})^2} \quad (B1)$$

$$I_{2\mu\nu} = \int_{-\pi}^{\pi} \frac{d^4k}{(2\pi)^4} \frac{\overset{\circ}{k}_\mu \sin(aq_\nu)}{(\widehat{k^2})^2 (\widehat{k+aq})^2} \int_{-\pi}^{\pi} \frac{d^4p}{(2\pi)^4} \frac{1}{\overset{\circ}{p}^2 (\overset{\circ}{p+k})^2} \quad (B2)$$

$$I_{3\mu\nu\rho\sigma} = \int_{-\pi}^{\pi} \frac{d^4k}{(2\pi)^4} \frac{\overset{\circ}{k}_\mu \overset{\circ}{k}_\nu}{(\widehat{k^2})^2 (\widehat{k+aq})^2} \int_{-\pi}^{\pi} \frac{d^4p}{(2\pi)^4} \frac{\sin(2p_\rho) \sin(2p_\sigma)}{(\overset{\circ}{p})^2 (\overset{\circ}{p+k})^2} \quad (B3)$$

$$I_{4\mu\nu\rho\sigma} = \int_{-\pi}^{\pi} \frac{d^4k}{(2\pi)^4} \frac{\overset{\circ}{k}_\mu \sin(aq_\nu)}{(\widehat{k^2})^2 (\widehat{k+aq})^2} \int_{-\pi}^{\pi} \frac{d^4p}{(2\pi)^4} \frac{\sin(2p_\rho) \sin(2p_\sigma)}{(\overset{\circ}{p})^2 (\overset{\circ}{p+k})^2} \quad (B4)$$

where $\widehat{p^2} = \sum_\mu \widehat{p}_\mu^2$, $\widehat{p}_\mu = 2 \sin(p_\mu/2)$, $\overset{\circ}{p}^2 = \sum_\mu \overset{\circ}{p}_\mu^2$, $\overset{\circ}{p}_\mu = \sin(p_\mu)$ and q is an external momentum. The crucial point is the presence of expressions like $\overset{\circ}{p}^2$ or $(\overset{\circ}{p+k})^2$ rather than $\widehat{p^2}$ or $(\widehat{p+k})^2$ in the denominators of the above integrals. This behaviour comes from the tree-level staggered fermion propagator. Also, the other crucial point is the fact that we cannot manipulate these integrals via subtractions of the form:

$$\frac{1}{\overset{\circ}{p}^2} = \frac{1}{\widehat{p}^2} + \left(\frac{1}{\overset{\circ}{p}^2} - \frac{1}{\widehat{p}^2} \right) \quad (B5)$$

in order to express them in terms of a standard tabulated integral plus additional terms which are more convergent; such a procedure is applicable, e.g., in the case of the Wilson fermion propagator $\left[1/(\overset{\circ}{p}^2 + r^2(\widehat{p^2})^2/4)\right]$ or in other less divergent integrals with staggered fermion propagators. The reason for which such a subtraction cannot be applied is the existence of potential IR singularities at all corners of the Brillouin zone (not only at zero momentum), in the staggered fermion propagator. Therefore, such a subtraction will not alleviate the divergent behaviour at the remaining corners of the Brillouin zone.

For the above integrals we followed a different approach. At first, we perform the substitution $p_\mu \rightarrow p'_\mu + \pi C_\mu$, where $-\pi/2 < p'_\mu < \pi/2$ and $C_\mu \in \{0, 1\}$, which is the same substitution that we applied to external momenta. Now the integration region for the innermost integral breaks up into 16 regions with range $[-\pi/2, \pi/2]$; the contributions from these regions are identical. To restore the initial range $[-\pi, \pi]$, we apply the following change of variables: $p'_\mu \rightarrow p''_\mu = 2p'_\mu$. Then we obtain:

$$I_{1\mu\nu} = 16 \int_{-\pi}^{\pi} \frac{d^4k}{(2\pi)^4} \frac{\overset{\circ}{k}_\mu \overset{\circ}{k}_\nu}{(\widehat{k^2})^2 (\widehat{k+aq})^2} \int_{-\pi}^{\pi} \frac{d^4p}{(2\pi)^4} \frac{1}{\overset{\circ}{p}^2 (\overset{\circ}{p+2k})^2} \quad (B6)$$

$$I_{2\mu\nu} = 16 \int_{-\pi}^{\pi} \frac{d^4k}{(2\pi)^4} \frac{\overset{\circ}{k}_\mu \sin(aq_\nu)}{(\widehat{k^2})^2 (\widehat{k+aq})^2} \int_{-\pi}^{\pi} \frac{d^4p}{(2\pi)^4} \frac{1}{\overset{\circ}{p}^2 (\overset{\circ}{p+2k})^2} \quad (B7)$$

$$I_{3\mu\nu\rho\sigma} = 64 \int_{-\pi}^{\pi} \frac{d^4k}{(2\pi)^4} \frac{\overset{\circ}{k}_\mu \overset{\circ}{k}_\nu}{(\widehat{k^2})^2 (\widehat{k+aq})^2} \int_{-\pi}^{\pi} \frac{d^4p}{(2\pi)^4} \frac{\overset{\circ}{p}_\rho \overset{\circ}{p}_\sigma}{(\overset{\circ}{p})^2 (\overset{\circ}{p+2k})^2} \quad (B8)$$

$$I_{4\mu\nu\rho\sigma} = 64 \int_{-\pi}^{\pi} \frac{d^4k}{(2\pi)^4} \frac{\overset{\circ}{k}_\mu \sin(aq_\nu)}{(\widehat{k^2})^2 (\widehat{k+aq})^2} \int_{-\pi}^{\pi} \frac{d^4p}{(2\pi)^4} \frac{\overset{\circ}{p}_\rho \overset{\circ}{p}_\sigma}{(\overset{\circ}{p})^2 (\overset{\circ}{p+2k})^2} \quad (B9)$$

where we omit the double prime from p . The above integrals are similar to standard divergent integrals, computed in Ref. [20]. The only difference is the presence of a factor of 2 in the denominators, i.e. $1/(\widehat{p+2k})^2$. This can be treated via subtraction methods. We define:

$$A(k) = \int_{-\pi}^{\pi} \frac{d^4 p}{(2\pi)^4} \frac{1}{\widehat{p^2} (\widehat{p+k})^2} \quad (\text{B10})$$

$$A_{\text{as}}(k) \equiv \frac{1}{(4\pi)^2} [-\ln(k^2) + 2] + P_2 \quad (\text{B11})$$

$$B_{\rho\sigma}(k) = \int_{-\pi}^{\pi} \frac{d^4 p}{(2\pi)^4} \frac{\overset{\circ}{p}_\rho \overset{\circ}{p}_\sigma}{(\widehat{p^2})^2 (\widehat{p+k})^2} \quad (\text{B12})$$

$$\widetilde{B}_{\rho\sigma}(2k) \equiv \frac{1}{2(4\pi)^2} \frac{\overset{\circ}{k}_\rho \overset{\circ}{k}_\sigma}{\widehat{k^2}} + \delta_{\rho\sigma} \left[\frac{1}{4} A(2k) - \frac{1}{32} P_1 \right] \quad (\text{B13})$$

where the values of the numerical constants P_1 and P_2 are noted in Ref. [20]. $A_{\text{as}}(k)$ and $\widetilde{B}_{\rho\sigma}(2k)$ are asymptotic values of $A(k)$ and $B_{\rho\sigma}(2k)$, respectively:

$$A(k) = A_{\text{as}}(k) + \mathcal{O}(k^2), \quad B_{\rho\sigma}(2k) = \widetilde{B}_{\rho\sigma}(2k) + \mathcal{O}(k^2) \quad (\text{B14})$$

The first two integrals $I_{1\mu\nu}$ and $I_{2\mu\nu}$ contain the quantity $A(2k)$ and the remaining two integrals $I_{3\mu\nu\rho\sigma}$ and $I_{4\mu\nu\rho\sigma}$ the quantity $B_{\rho\sigma}(2k)$. We apply the following subtractions:

$$A(2k) = A(k) + [A_{\text{as}}(2k) - A_{\text{as}}(k)] + [A(2k) - A(k) - A_{\text{as}}(2k) + A_{\text{as}}(k)] \quad (\text{B15})$$

$$B_{\rho\sigma}(2k) = \widetilde{B}_{\rho\sigma}(2k) + [B_{\rho\sigma}(2k) - \widetilde{B}_{\rho\sigma}(2k)] \quad (\text{B16})$$

Integrals $I_{1\mu\nu}$ and $I_{2\mu\nu}$ separate into 3 sub-integrals. The first sub-integral with the quantity $A(k)$ is already computed in Ref. [20] (for $I_{1\mu\nu}$) or can be converted into standard divergent integrals of Ref. [20] using integration by parts (for $I_{2\mu\nu}$). The second sub-integral with the quantity $[A_{\text{as}}(2k) - A_{\text{as}}(k)] = -\ln 4/(4\pi)^2$ is a one loop divergent integral computed in Ref. [20] or [21]. The third sub-integral with the quantity $[A(2k) - A(k) - A_{\text{as}}(2k) + A_{\text{as}}(k)] = \mathcal{O}(k^2)$ is convergent and so we can integrate it numerically for $a \rightarrow 0$ (In particular, it gives zero for $I_{2\mu\nu}$). Also, integrals $I_{3\mu\nu\rho\sigma}$ and $I_{4\mu\nu\rho\sigma}$ separate into 2 sub-integrals. The first sub-integral with the quantity $\widetilde{B}_{\rho\sigma}(2k)$ gives expressions which can be converted into standard integrals of Refs. [20–23] or into the above $I_{1\mu\nu}$, $I_{2\mu\nu}$ integrals. The second sub-integral with the quantity $[B_{\rho\sigma}(2k) - \widetilde{B}_{\rho\sigma}(2k)] = \mathcal{O}(k^2)$ is convergent and so we can integrate it numerically for $a \rightarrow 0$ (In particular, it gives zero for $I_{4\mu\nu\rho\sigma}$). Therefore, according to the above manipulations, the final expressions for the four integrals are given by:

$$\begin{aligned} I_{1\mu\nu} &= \left\{ \frac{2}{(2\pi)^4} \left[-\ln(a^2 q^2) + \frac{3}{2} - \ln 4 \right] + \frac{1}{2\pi^2} P_2 \right\} \frac{q_\mu q_\nu}{q^2} \\ &+ \delta_{\mu\nu} \left\{ \frac{2}{(4\pi)^4} \left[\ln(a^2 q^2) \right]^2 - \frac{1}{4\pi^2} \left[P_2 + \frac{1}{(4\pi)^2} \left(\frac{5}{2} - \ln 4 \right) \right] \ln(a^2 q^2) - \frac{1}{4\pi^2} \left[P_2 + \frac{3}{2(4\pi)^2} \ln 4 \right] + 4X_2 + G_1 \right\} \\ &+ \mathcal{O}(a^2 q^2) \end{aligned} \quad (\text{B17})$$

$$I_{2\mu\nu} = \left\{ \frac{1}{(2\pi)^4} \left[\ln(a^2 q^2) - 2 + \ln 4 \right] - \frac{1}{\pi^2} P_2 \right\} \frac{q_\mu q_\nu}{q^2} + \mathcal{O}(a^2 q^2) \quad (\text{B18})$$

$$\begin{aligned} I_{3\mu\nu\rho\sigma} &= \frac{1}{3(2\pi)^4} \frac{q_\mu q_\nu q_\rho q_\sigma}{q^4} + \delta_{\rho\sigma} \left\{ \frac{2}{(2\pi)^4} \left[-\ln(a^2 q^2) + \frac{5}{3} - \ln 4 \right] - \frac{1}{(4\pi)^2} (P_1 - 8P_2) \right\} \frac{q_\mu q_\nu}{q^2} \\ &+ \frac{1}{12(2\pi)^4} \left\{ \delta_{\mu\nu} \frac{q_\rho q_\sigma}{q^2} + \delta_{\mu\rho} \frac{q_\nu q_\sigma}{q^2} + \delta_{\mu\sigma} \frac{q_\nu q_\rho}{q^2} + \delta_{\nu\rho} \frac{q_\mu q_\sigma}{q^2} + \delta_{\nu\sigma} \frac{q_\mu q_\rho}{q^2} \right\} \\ &+ \delta_{\mu\nu} \delta_{\rho\sigma} \left\{ \frac{2}{(4\pi)^4} \left[\ln(a^2 q^2) \right]^2 - \frac{1}{4\pi^2} \left[P_2 - \frac{1}{8} P_1 + \frac{1}{(4\pi)^2} \left(\frac{51}{2} - \ln 4 \right) \right] \ln(a^2 q^2) \right. \\ &\quad \left. - \frac{1}{4\pi^2} \left[\left(\frac{1}{3} - \ln 4 \right) P_2 - \frac{11}{144} P_1 + \frac{3}{2(4\pi)^2} \left(\frac{1}{27} - \ln 4 \right) \right] - \frac{1}{2} P_1 P_2 + 4X_2 + G_1 + G_3 \right\} \\ &+ (\delta_{\mu\rho} \delta_{\nu\sigma} + \delta_{\mu\sigma} \delta_{\nu\rho}) \left\{ \frac{1}{(12\pi)^4} \left[-\ln(a^2 q^2) + \frac{1}{6} \right] + \frac{1}{6\pi^2} (P_1 + 3P_2) + G_2 \right\} \\ &+ \delta_{\mu\nu\rho\sigma} \left\{ \frac{1}{(2\pi)^4} + \frac{1}{2(4\pi)^2} - \frac{1}{3\pi^2} P_1 + G_4 \right\} + \mathcal{O}(a^2 q^2) \end{aligned} \quad (\text{B19})$$

$$\begin{aligned}
I_{4\mu\nu\rho\sigma} &= -\frac{1}{2(2\pi)^4} \frac{q_\mu q_\nu q_\rho q_\sigma}{q^4} - \frac{4}{(4\pi)^4} \left\{ \delta_{\mu\rho} \frac{q_\nu q_\sigma}{q^2} + \delta_{\mu\sigma} \frac{q_\nu q_\rho}{q^2} \right\} \\
&+ \delta_{\rho\sigma} \left\{ \frac{1}{(2\pi)^4} \left[\ln(a^2 q^2) - \frac{9}{4} \right] - \frac{1}{2(2\pi)^2} (P_1 - 8P_2) \right\} \frac{q_\mu q_\nu}{q^2} + \mathcal{O}(a^2 q^2)
\end{aligned} \tag{B20}$$

where P_1, P_2, X_2 are given in Ref. [20] and $G_1 - G_4$ are given below:

$$G_1 = 0.000803016(6) \tag{B21}$$

$$G_2 = -0.0006855532(7) \tag{B22}$$

$$G_3 = 0.00098640(7) \tag{B23}$$

$$G_4 = 0.00150252(2) \tag{B24}$$

-
- [1] M. Constantinou, M. Hadjiantonis, and H. Panagopoulos, PoS **LATTICE2014**, 298 (2014), [arXiv:1411.6990].
- [2] A. J. Chambers, R. Horsley, Y. Nakamura, H. Perlt, P. E. L. Rakow, G. Schierholz, A. Schiller, and J. M. Zanotti (QCDSF Collaboration) (2014), [arXiv:1410.3078].
- [3] A. Skouroupathis and H. Panagopoulos, Phys. Rev. **D76**, 094514 (2007), [arXiv:0707.2906].
- [4] A. Skouroupathis and H. Panagopoulos, Phys. Rev. **D79**, 094508 (2009), [arXiv:0811.4264].
- [5] M. Brambilla, F. Di Renzo, and M. Hasegawa (2014), [arXiv:1402.6581].
- [6] Y. Aoki, Z. Fodor, S. D. Katz, and K. Szabo, JHEP **0601**, 089 (2006), [hep-lat/0510084].
- [7] S. Borsányi, Z. Fodor, S. Katz, S. Krieg, C. Ratti, et al. (Wuppertal-Budapest Collaboration), J. Phys. **G38**, 124060 (2011), [arXiv:1109.5030].
- [8] A. Bazavov, C. Bernard, C. DeTar, W. Freeman, S. Gottlieb, et al. (MILC Collaboration) (2012), [arXiv:1212.4768].
- [9] M. Constantinou, M. Costa, and H. Panagopoulos, Phys. Rev. **D88**, 034504 (2013), [arXiv:1305.1870].
- [10] R. Horsley, H. Perlt, P. E. L. Rakow, G. Schierholz, and A. Schiller, Phys. Rev. **D78**, 054504 (2008), [arXiv:0807.0345].
- [11] C. Morningstar and M. J. Peardon, Phys. Rev. **D69**, 054501 (2004), [hep-lat/0311018].
- [12] R. Horsley, H. Perlt, P. E. L. Rakow, G. Schierholz, and A. Schiller (QCDSF), Nucl. Phys. **B693**, 3 (2004), [Erratum: Nucl. Phys. B713, 601(2005)], [hep-lat/0404007].
- [13] A. Patel and S. R. Sharpe, Nucl. Phys. **B395**, 701 (1993), [hep-lat/9210039].
- [14] S. A. Larin, Phys. Lett. **B303**, 113 (1993), [hep-ph/9302240].
- [15] H. Panagopoulos, A. Skouroupathis, and A. Tsapalis, Phys. Rev. **D73**, 054511 (2006), [hep-lat/0601009].
- [16] M. Constantinou, PoS **LATTICE2014**, 001 (2015), [arXiv:1411.0078].
- [17] A. Hasenfratz and F. Knechtli, Phys. Rev. **D64**, 034504 (2001), [hep-lat/0103029].
- [18] S. Capitani, S. Durr, and C. Hoelbling, JHEP **11**, 028 (2006), [hep-lat/0607006].
- [19] K. Orginos, D. Toussaint, and R. L. Sugar (MILC), Phys. Rev. **D60**, 054503 (1999), [hep-lat/9903032].
- [20] M. Lüscher and P. Weisz, Nucl. Phys. **B452**, 234 (1995), [hep-lat/9505011].
- [21] K. Chetyrkin and F. Tkachov, Nucl. Phys. **B192**, 159 (1981).
- [22] H. Panagopoulos and E. Vicari, Nucl. Phys. **B332**, 261 (1990).
- [23] R. Ellis and G. Martinelli, Nucl. Phys. **B235**, 93 (1984).

ADDENDUM: LIST OF CONVERSION RELATIONS BETWEEN RI' , RI' -ALTERNATIVE AND \overline{MS} SCHEMES

The two-loop difference $Z_\Gamma^{singlet} - Z_\Gamma^{nonsinglet}$ is renormalization scheme independent for all operators Γ , except for the axial vector case. There are two factors contributing to this scheme dependence: On one hand, the conversion factor Z_5^A between RI' and \overline{MS} differs for the singlet and nonsinglet operators (see Eqs. 27,29,30); on the other hand, non-identical contributions of the form $\gamma_5 q_\mu \not{q}/q^2$ in the Green's functions for the singlet and nonsinglet axial vector operators lead to a nontrivial conversion between the RI' and RI' -alternative schemes, as shown in Eq. (33). In order to clarify scheme dependence, we list below all relevant conversion factors relating the RI' , RI' -alternative and \overline{MS} schemes. Given that the conversion factors are regularization independent, the renormalization functions Z_Γ appearing below may be evaluated in any regularization scheme.

A. Conversion factors between RI' and \overline{MS} schemes

$$C_\Gamma^{\overline{MS},RI'} \equiv C_\Gamma \equiv \frac{Z_\Gamma^{RI'}}{Z_\Gamma^{\overline{MS}}} \quad (36)$$

$$C_{S(singlet)}^{\overline{MS},RI'} = C_{S(nonsinglet)}^{\overline{MS},RI'} = 1 + \frac{g_{RI'}^2}{(4\pi)^2} c_F (\alpha_{\overline{MS}} + 4) + \frac{g_{RI'}^4}{24(4\pi)^4} c_F \left[(24 \alpha_{\overline{MS}}^2 + 96 \alpha_{\overline{MS}} - 288 \zeta(3) + 57) c_F + 166 N_f - (18 \alpha_{\overline{MS}}^2 + 84 \alpha_{\overline{MS}} - 432 \zeta(3) + 1285) N_c \right] + \mathcal{O}(g_{RI'}^6) \quad (37)$$

$$C_{P(singlet/nonsinglet)}^{\overline{MS},RI'} = C_{S(singlet/nonsinglet)}^{\overline{MS},RI'} Z_5^P \quad (38)$$

$$C_{V(singlet)}^{\overline{MS},RI'} = C_{V(nonsinglet)}^{\overline{MS},RI'} = 1 + \mathcal{O}(g_{RI'}^8) \quad (39)$$

$$C_{A(singlet/nonsinglet)}^{\overline{MS},RI'} = C_{V(singlet/nonsinglet)}^{\overline{MS},RI'} Z_5^{A(singlet/nonsinglet)} \quad (40)$$

$$C_{T(singlet)}^{\overline{MS},RI'} = C_{T(nonsinglet)}^{\overline{MS},RI'} = 1 + \frac{g_{RI'}^2}{(4\pi)^2} c_F \alpha_{\overline{MS}} + \frac{g_{RI'}^4}{216(4\pi)^4} c_F \left[(216 \alpha_{\overline{MS}}^2 + 4320 \zeta(3) - 4815) c_F + 626 N_f + (162 \alpha_{\overline{MS}}^2 + 756 \alpha_{\overline{MS}} - 3024 \zeta(3) + 5987) N_c \right] + \mathcal{O}(g_{RI'}^6) \quad (41)$$

where Z_5^P and $Z_5^{A(singlet/nonsinglet)}$ are given in Eqs. (28 - 30) and $\zeta(x)$ is Riemann's zeta function. The conversion of gauge parameter α between the two schemes is given by:

$$\alpha_{RI'} = \frac{\alpha_{\overline{MS}}}{C_{A_\mu}^{\overline{MS},RI'}} \quad (42)$$

where the conversion factor $C_{A_\mu}^{\overline{MS},RI'}$ for the gluon field A_μ is given by¹

$$C_{A_\mu}^{\overline{MS},RI'} \equiv \frac{Z_{A_\mu}^{RI'}}{Z_{A_\mu}^{\overline{MS}}} = 1 + \frac{g_{RI'}^2}{36(4\pi)^2} \left[(9 \alpha_{\overline{MS}}^2 + 18 \alpha_{\overline{MS}} + 97) N_c - 40 N_f \right] + \mathcal{O}(g_{RI'}^4) \quad (43)$$

The renormalized coupling constant in the RI' scheme, $g_{RI'}$, is conventionally taken to have the same value as in the \overline{MS} scheme, $g_{\overline{MS}}$.

¹ Not to be confused with the conversion factor $C_A^{\overline{MS},RI'}$ for the axial vector operator!

B. Conversion factors between RI' and RI' -ALTERNATIVE schemes

$$C_{\Gamma}^{RI',RI'alter} \equiv \frac{Z_{\Gamma}^{RI'alter}}{Z_{\Gamma}^{RI'}} \quad (44)$$

$$C_{S(singlet)}^{RI',RI'alter} = C_{S(nonsinglet)}^{RI',RI'alter} = C_{P(singlet)}^{RI',RI'alter} = C_{P(nonsinglet)}^{RI',RI'alter} = 1 \quad (45)$$

$$C_{V(singlet)}^{RI',RI'alter} = C_{V(nonsinglet)}^{RI',RI'alter} = C_{A(nonsinglet)}^{RI',RI'alter} = 1 - \frac{g_{RI'}^4}{(4\pi)^4} c_F \left(\frac{3}{4} c_F - \frac{251}{36} N_c + \frac{19}{18} N_f \right) + \mathcal{O}(g_{RI'}^6) \quad (46)$$

$$C_{A(singlet)}^{RI',RI'alter} = 1 - \frac{g_{RI'}^4}{(4\pi)^4} c_F \left(\frac{3}{4} c_F - \frac{251}{36} N_c + \frac{1}{18} N_f \right) + \mathcal{O}(g_{RI'}^6) \quad (47)$$

$$C_{T(singlet)}^{RI',RI'alter} = C_{T(nonsinglet)}^{RI',RI'alter} = 1 + \mathcal{O}(g_{RI'}^6) \quad (48)$$

C. Conversion between RI' -ALTERNATIVE and \overline{MS} schemes

$$Z_{\Gamma(singlet/nonsinglet)}^{\overline{MS}} = \frac{Z_{\Gamma(singlet/nonsinglet)}^{RI'alter}}{C_{\Gamma(singlet/nonsinglet)}^{\overline{MS},RI'} C_{\Gamma(singlet/nonsinglet)}^{RI',RI'alter}} \quad (49)$$

D. Relation of $Z_{\Gamma}^{singlet} - Z_{\Gamma}^{nonsinglet}$ between the RI' -ALTERNATIVE and RI' schemes

$$Z_{\Gamma}^{RI'alter(singlet)} - Z_{\Gamma}^{RI'alter(nonsinglet)} = Z_{\Gamma}^{RI'(singlet)} - Z_{\Gamma}^{RI'(nonsinglet)} \quad (\Gamma = S, P) \quad (50)$$

$$Z_{\Gamma}^{RI'alter(singlet)} - Z_{\Gamma}^{RI'alter(nonsinglet)} = Z_{\Gamma}^{RI'(singlet)} - Z_{\Gamma}^{RI'(nonsinglet)} + \mathcal{O}(g_o^6) \quad (\Gamma = V, T) \quad (51)$$

$$Z_A^{RI'alter(singlet)} - Z_A^{RI'alter(nonsinglet)} = Z_A^{RI'(singlet)} - Z_A^{RI'(nonsinglet)} + \frac{g_o^4}{(4\pi)^4} c_F N_f + \mathcal{O}(g_o^6) \quad (52)$$

E. Relation of $Z_{\Gamma}^{singlet} - Z_{\Gamma}^{nonsinglet}$ between the \overline{MS} and RI' schemes

$$Z_{\Gamma}^{\overline{MS}(singlet)} - Z_{\Gamma}^{\overline{MS}(nonsinglet)} = Z_{\Gamma}^{RI'(singlet)} - Z_{\Gamma}^{RI'(nonsinglet)} + \mathcal{O}(g_o^6) \quad (\Gamma = S, P, V, T) \quad (53)$$

$$Z_A^{\overline{MS}(singlet)} - Z_A^{\overline{MS}(nonsinglet)} = Z_A^{RI'(singlet)} - Z_A^{RI'(nonsinglet)} + \frac{g_o^4}{(4\pi)^4} \left(-\frac{3}{2} c_F N_f \right) + \mathcal{O}(g_o^6) \quad (54)$$

F. Relation of $Z_{\Gamma}^{singlet} - Z_{\Gamma}^{nonsinglet}$ between the \overline{MS} and RI' -ALTERNATIVE schemes

$$Z_{\Gamma}^{\overline{MS}(singlet)} - Z_{\Gamma}^{\overline{MS}(nonsinglet)} = Z_{\Gamma}^{RI'alter(singlet)} - Z_{\Gamma}^{RI'alter(nonsinglet)} + \mathcal{O}(g_o^6) \quad (\Gamma = S, P, V, T) \quad (55)$$

$$Z_A^{\overline{MS}(singlet)} - Z_A^{\overline{MS}(nonsinglet)} = Z_A^{RI'alter(singlet)} - Z_A^{RI'alter(nonsinglet)} + \frac{g_o^4}{(4\pi)^4} \left(-\frac{5}{2} c_F N_f \right) + \mathcal{O}(g_o^6) \quad (56)$$